



**HAL**  
open science

## Palaeohydrological changes recorded from a small Moroccan Middle Atlas pond during the last 6000 cal. yr BP: a multi-proxy study

Hanane Id Abdellah, Laurence Vidal, Abdelfattah Benkaddour, Ali Rhoujjati, Guillaume Jouve, Tachikawa Kazuyo, Corinne Sonzogni, Florence Sylvestre, Christine Paillès, Jean-Charles Mazure

### ► To cite this version:

Hanane Id Abdellah, Laurence Vidal, Abdelfattah Benkaddour, Ali Rhoujjati, Guillaume Jouve, et al.. Palaeohydrological changes recorded from a small Moroccan Middle Atlas pond during the last 6000 cal. yr BP: a multi-proxy study. *Journal of Paleolimnology*, 2021, 10.1007/s10933-020-00166-6 . hal-03122512

**HAL Id: hal-03122512**

**<https://hal.science/hal-03122512>**

Submitted on 27 Jan 2021

**HAL** is a multi-disciplinary open access archive for the deposit and dissemination of scientific research documents, whether they are published or not. The documents may come from teaching and research institutions in France or abroad, or from public or private research centers.

L'archive ouverte pluridisciplinaire **HAL**, est destinée au dépôt et à la diffusion de documents scientifiques de niveau recherche, publiés ou non, émanant des établissements d'enseignement et de recherche français ou étrangers, des laboratoires publics ou privés.



Distributed under a Creative Commons Attribution - NonCommercial - NoDerivatives 4.0 International License

Dear Author,

Here are the proofs of your article.

- You can submit your corrections **online**, via **e-mail** or by **fax**.
- For **online** submission please insert your corrections in the online correction form. Always indicate the line number to which the correction refers.
- You can also insert your corrections in the proof PDF and **email** the annotated PDF.
- For fax submission, please ensure that your corrections are clearly legible. Use a fine black pen and write the correction in the margin, not too close to the edge of the page.
- Remember to note the **journal title**, **article number**, and **your name** when sending your response via e-mail or fax.
- **Check** the metadata sheet to make sure that the header information, especially author names and the corresponding affiliations are correctly shown.
- **Check** the questions that may have arisen during copy editing and insert your answers/ corrections.
- **Check** that the text is complete and that all figures, tables and their legends are included. Also check the accuracy of special characters, equations, and electronic supplementary material if applicable. If necessary refer to the *Edited manuscript*.
- The publication of inaccurate data such as dosages and units can have serious consequences. Please take particular care that all such details are correct.
- Please **do not** make changes that involve only matters of style. We have generally introduced forms that follow the journal's style. Substantial changes in content, e.g., new results, corrected values, title and authorship are not allowed without the approval of the responsible editor. In such a case, please contact the Editorial Office and return his/her consent together with the proof.
- If we do not receive your corrections **within 48 hours**, we will send you a reminder.
- Your article will be published **Online First** approximately one week after receipt of your corrected proofs. This is the **official first publication** citable with the DOI. **Further changes are, therefore, not possible.**
- The **printed version** will follow in a forthcoming issue.

#### **Please note**

After online publication, subscribers (personal/institutional) to this journal will have access to the complete article via the DOI using the URL: [http://dx.doi.org/\[DOI\]](http://dx.doi.org/[DOI]).

If you would like to know when your article has been published online, take advantage of our free alert service. For registration and further information go to: <http://www.link.springer.com>.

Due to the electronic nature of the procedure, the manuscript and the original figures will only be returned to you on special request. When you return your corrections, please inform us if you would like to have these documents returned.

# Metadata of the article that will be visualized in OnlineFirst

---

ArticleTitle	Palaeohydrological changes recorded from a small Moroccan Middle Atlas pond during the last 6000 cal. yr BP: a multi-proxy study
--------------	--

---

Article Sub-Title

---

Article CopyRight	The Author(s), under exclusive licence to Springer Nature B.V. part of Springer Nature (This will be the copyright line in the final PDF)
-------------------	--

---

Journal Name

---

Corresponding Author	Family Name	<b>Abdellah</b>
	Particle	
	Given Name	<b>Hanane Id</b>
	Suffix	
	Division	
	Organization	Laboratoire Géoressources
	Address	Marrakech, Morocco
	Division	CNRS, IRD, INRAE, Coll France, CEREGE
	Organization	Aix-Marseille University
	Address	Aix-en-Provence, France
	Division	
	Organization	
	Address	
	Phone	
	Fax	
	Email	hananeidabdellah@gmail.com
	URL	
	ORCID	

---

Author	Family Name	<b>Vidal</b>
	Particle	
	Given Name	<b>Laurence</b>
	Suffix	
	Division	CNRS, IRD, INRAE, Coll France, CEREGE
	Organization	Aix-Marseille University
	Address	Aix-en-Provence, France
	Phone	
	Fax	
	Email	vidal@cerege.fr
	URL	
	ORCID	

---

Author	Family Name	<b>Benkaddour</b>
	Particle	
	Given Name	<b>Abdelfattah</b>
	Suffix	

Division Laboratoire Géoressources, Faculté des Sciences et Techniques, CNRST (URAC 42)  
Organization Université Cadi Ayyad  
Address Marrakech, Morocco  
Phone  
Fax  
Email a.benkaddour@uca.ac.ma  
URL  
ORCID

---

Author Family Name **Rhoujjati**  
Particle  
Given Name **Ali**  
Suffix  
Division Laboratoire Géoressources, Faculté des Sciences et Techniques, CNRST (URAC 42)  
Organization Université Cadi Ayyad  
Address Marrakech, Morocco  
Phone  
Fax  
Email a.rhoujjati@uca.ac.ma  
URL  
ORCID

---

Author Family Name **Jouve**  
Particle  
Given Name **Guillaume**  
Suffix  
Division  
Organization iXblue Sonar Systems Division  
Address La Ciotat, France  
Phone  
Fax  
Email guillaume.jouve@ixblue.com  
URL  
ORCID

---

Author Family Name **Tachikawa**  
Particle  
Given Name **Kazuyo**  
Suffix  
Division  
Organization Laboratoire Géoressources  
Address Marrakech, Morocco  
Division CNRS, IRD, INRAE, Coll France, CEREGE  
Organization Aix-Marseille University  
Address Aix-en-Provence, France  
Phone  
Fax

Email kazuyo@cerege.fr  
URL  
ORCID

---

Author Family Name **Sonzogni**  
Particle  
Given Name **Corinne**  
Suffix  
Division CNRS, IRD, INRAE, Coll France, CEREGE  
Organization Aix-Marseille University  
Address Aix-en-Provence, France  
Phone  
Fax  
Email sonzoni@cerege.fr  
URL  
ORCID

---

Author Family Name **Mazur**  
Particle  
Given Name **Jean-Charles**  
Suffix  
Division CNRS, IRD, INRAE, Coll France, CEREGE  
Organization Aix-Marseille University  
Address Aix-en-Provence, France  
Phone  
Fax  
Email mazur@cerege.fr  
URL  
ORCID

---

Author Family Name **Pailès**  
Particle  
Given Name **Christine**  
Suffix  
Division CNRS, IRD, INRAE, Coll France, CEREGE  
Organization Aix-Marseille University  
Address Aix-en-Provence, France  
Phone  
Fax  
Email pailles@cerege.fr  
URL  
ORCID

---

Author Family Name **Sylvestre**  
Particle  
Given Name **Florence**  
Suffix  
Division CNRS, IRD, INRAE, Coll France, CEREGE  
Organization Aix-Marseille University

Address Aix-en-Provence, France  
Phone  
Fax  
Email sylvestre@cerege.fr  
URL  
ORCID

---

Schedule	Received	13 September 2019
	Revised	
	Accepted	5 December 2020

---

**Abstract** The perennial and seasonal wetland diversity of the Moroccan Middle Atlas region provides a valuable “test-bed” for understanding the response of different hydrosystems to climatic variations. A multiproxy study, based on sedimentological descriptions, together with mineralogy, carbonate content, XRF core scanning and biological proxies supported by AMS <sup>14</sup>C dates, were applied to the 3-m-long core extracted from “Flowers Marsh”, a small Middle Atlas pond. This approach provides evidence for a continuous paleohydrological and paleoenvironmental record during the Mid- to Late Holocene. The investigated aquatic system evolved from a dry or very shallow waterbody towards a system with a progressively rising water level. The dominance of the detrital fraction with poor preservation of bioindicators and eroded pollen, indicate the existence of an ephemeral waterbody from 6000 cal. yr BP until a transitional phase characterized by new sedimentological facies and the appearance of ostracods around 2300 cal. yr BP. This transition, ending at 2000 cal. yr BP, is interpreted as a flooding phase leading to an ephemeral lake. It is certainly fed by the excess water from the nearby Aguelmam Azigza Lake during its high level period. Afterwards, enhanced organic matter deposition and the appearance of well-preserved diatoms until 1400 cal. yr BP corroborate a high water-level trend. Endogenic carbonate to detrital fraction ratios indicate fluctuating, but generally shallow, water levels from 1400 cal. yr BP until 650 cal. yr BP when a relatively rapid rise in water level occurred. Flowers Marsh data are, generally, consistent with most of the existing regional records. The highstand period recorded between 2000 and 1400 cal. yr is a common feature extending to more distant sites from the northern Mediterranean. It corresponds to the wetter Iberian-Roman period. Fluctuating shallow water levels recorded since 1400 cal. yr BP to now could be linked to drier/wetter phases associated with the Medieval Climate Anomaly and the Little Ice Age (650–150 cal. yr BP) respectively, in the western Mediterranean realm. The present study demonstrates the ability of Flowers Marsh to record valuable palaeohydrological changes since the Mid-Holocene and confirms the high sensitivity of Middle Atlas hydrosystems to climatic changes.

---

**Keywords (separated by '-')** Middle Atlas - Palaeohydrology - Mid- to Late-Holocene - Lacustrine sediment - Climatic changes

---

**Footnote Information** **Supporting Information** The online version of this article (<https://doi.org/10.1007/s10933-020-00166-6>) contains supplementary material, which is available to authorized users.

---



2 **Palaeohydrological changes recorded from a small**  
3 **Moroccan Middle Atlas pond during the last 6000 cal. yr**  
4 **BP: a multi-proxy study**

5 **Hanane Id Abdellah · Laurence Vidal · Abdelfattah Benkaddour ·**  
6 **Ali Rhoujjati · Guillaume Jouve · Kazuyo Tachikawa · Corinne Sonzogni ·**  
7 **Jean-Charles Mazur · Christine Paillès · Florence Sylvestre**

8 Received: 13 September 2019 / Accepted: 5 December 2020  
9 © The Author(s), under exclusive licence to Springer Nature B.V. part of Springer Nature 2020

10 **Abstract** The perennial and seasonal wetland diver-  
11 sity of the Moroccan Middle Atlas region provides a  
12 valuable “test-bed” for understanding the response of  
13 different hydrosystems to climatic variations. A  
14 multiproxy study, based on sedimentological descrip-  
15 tions, together with mineralogy, carbonate content,  
16 XRF core scanning and biological proxies supported  
17 by AMS <sup>14</sup>C dates, were applied to the 3-m-long core  
18 extracted from “Flowers Marsh”, a small Middle  
19 Atlas pond. This approach provides evidence for a

continuous paleohydrological and paleoenvironmen- 20  
tal record during the Mid- to Late Holocene. The 21  
investigated aquatic system evolved from a dry or very 22  
shallow waterbody towards a system with a progres- 23  
sively rising water level. The dominance of the detrital 24  
fraction with poor preservation of bioindicators and 25  
eroded pollen, indicate the existence of an ephemeral 26  
waterbody from 6000 cal. yr BP until a transitional 27  
phase characterized by new sedimentological facies 28  
and the appearance of ostracods around 2300 cal. yr 29  
BP. This transition, ending at 2000 cal. yr BP, is 30  
interpreted as a flooding phase leading to an ephemeral 31  
lake. It is certainly fed by the excess water from the 32

A1 **Supporting Information** The online version of this article  
A2 (<https://doi.org/10.1007/s10933-020-00166-6>) contains sup-  
A3 plementary material, which is available to authorized users.

A4 H. I. Abdellah (✉) · K. Tachikawa  
A5 Laboratoire Géoressources, Marrakech, Morocco  
A6 e-mail: hananeidabdellah@gmail.com

A7 K. Tachikawa  
A8 e-mail: kazuyo@cerege.fr

A9 H. I. Abdellah · L. Vidal · K. Tachikawa ·  
A10 C. Sonzogni · J.-C. Mazur · C. Paillès · F. Sylvestre  
A11 CNRS, IRD, INRAE, Coll France, CEREGE, Aix-  
A12 Marseille University, Aix-en-Provence, France  
A13 e-mail: vidal@cerege.fr

A14 C. Sonzogni  
A15 e-mail: sonzogni@cerege.fr

A16 J.-C. Mazur  
A17 e-mail: mazur@cerege.fr

A18 C. Paillès  
A19 e-mail: pailles@cerege.fr

A20 F. Sylvestre  
A21 e-mail: sylvestre@cerege.fr

A22 A. Benkaddour · A. Rhoujjati  
A23 Laboratoire Géoressources, Faculté des Sciences et  
A24 Techniques, CNRST (URAC 42), Université Cadi Ayyad,  
A25 Marrakech, Morocco  
A26 e-mail: a.benkaddour@uca.ac.ma

A27 A. Rhoujjati  
A28 e-mail: a.rhoujjati@uca.ac.ma

A29 G. Jouve  
A30 iXblue Sonar Systems Division, La Ciotat, France  
A31 e-mail: guillaume.jouve@ixblue.com

33 nearby Aguelmam Azigza Lake during its high level  
 34 period. Afterwards, enhanced organic matter deposi-  
 35 tion and the appearance of well-preserved diatoms  
 36 until 1400 cal. yr BP corroborate a high water-level  
 37 trend. Endogenic carbonate to detrital fraction ratios  
 38 indicate fluctuating, but generally shallow, water  
 39 levels from 1400 cal. yr BP until 650 cal. yr BP when  
 40 a relatively rapid rise in water level occurred. Flowers  
 41 Marsh data are, generally, consistent with most of the  
 42 existing regional records. The highstand period  
 43 recorded between 2000 and 1400 cal. yr is a common  
 44 feature extending to more distant sites from the  
 45 northern Mediterranean. It corresponds to the wetter  
 46 Iberian-Roman period. Fluctuating shallow water  
 47 levels recorded since 1400 cal. yr BP to now could  
 48 be linked to drier/wetter phases associated with the  
 49 Medieval Climate Anomaly and the Little Ice Age  
 50 (650– 150 cal. yr BP) respectively, in the western  
 51 Mediterranean realm. The present study demonstrates  
 52 the ability of Flowers Marsh to record valuable  
 53 palaeohydrological changes since the Mid-Holocene  
 54 and confirms the high sensitivity of Middle Atlas  
 55 hydrosystems to climatic changes.

56 **Keywords** Middle Atlas · Palaeohydrology · Mid- to  
 57 Late-Holocene · Lacustrine sediment · Climatic  
 58 changes

## 59 Introduction

60 The Mediterranean basin is one of the most sensitive  
 61 areas to climate fluctuations (Giorgi 2006). Future  
 62 climate change projections highlight the exposure of  
 63 the Western Mediterranean region to increased heat  
 64 and drought stress (Solomon et al. 2009; Born et al.  
 65 2010). The Middle Atlas region is considered to be the  
 66 main water reservoir of Morocco. This region is host to  
 67 a variety of perennial and semi-permanent wetlands  
 68 including natural lakes, rivers and springs. These  
 69 water resources are relied upon to meet the agricultural  
 70 and domestic needs of the region. During recent  
 71 decades, numerous lakes of the karstified Middle Atlas  
 72 region experienced a significant water deficit as a  
 73 result of recurrent droughts and human overexploita-  
 74 tion, including: Dayet Aoua (Sayad and Chakiri 2010),  
 75 Aguelmam Sidi Ali (Sayad et al. 2011), Ifrah Lake  
 76 (Etebaai et al. 2012) and Aguelmam Azigza (Adallal  
 77 et al. 2019). Examining the past history of lakes in the  
 78 Middle Atlas region can elucidate the prospective

79 impacts of combined climate change and anthro-  
 80 pogenic activity on the hydrological behavior of these  
 81 lacustrine systems.

82 Lake sediments have the potential to allow inves-  
 83 tigation of temporal paleohydrological trends under  
 84 various environmental conditions. Lacustrine  
 85 sequences from Middle Atlas wetlands are ideally  
 86 suited to understanding the response of Mediterranean  
 87 semi-arid environments and hydrosystems to climatic  
 88 changes because of the small size of their basins, and  
 89 because their evolution and sedimentation are directly  
 90 influenced by regional hydrologic changes (Lamb and  
 91 van der Kaars 1995). Pioneering paleoenvironmental  
 92 investigations have demonstrated the high potential of  
 93 Middle Atlas lake sediments as archives of climate  
 94 variability (Martin 1981; Lamb et al. 1989). The  
 95 number of available paleoclimatic and paleoenviron-  
 96 mental reconstructions conducted on lacustrine  
 97 sequences from the region has greatly increased in  
 98 the last few decades. Most of these records cover the  
 99 last glacial period (Rhoujjati et al. 2010; Nour El Bait  
 100 et al. 2014; Tabel et al. 2016) and the early Holocene  
 101 (Barker et al. 1994; Cheddadi et al. 1998; Lamb and  
 102 van der Kaars 1995; Campbell et al. 2017; Zielhofer  
 103 et al. 2017). The last few millennia are particularly  
 104 interesting owing to the fact that the main boundary  
 105 conditions were similar to present-day climate con-  
 106 figurations and detailed regional palaeoclimatic recon-  
 107 structions can be compared to current climate change  
 108 processes (Corella et al. 2011; Brisset et al. 2019).  
 109 However, records spanning the Mid-Late Holocene  
 110 period are rather scarce in the Middle Atlas region  
 111 (Damnati et al. 2015; Nour El Bait et al. 2016). Nour  
 112 El Bait et al. (2016) demonstrated that climate has  
 113 remained relatively stable over the last 6000 cal. yr BP  
 114 with a trend of aridity and warming towards the  
 115 present. Results obtained from lacustrine terraces at  
 116 three Middle Atlas lakes indicate high lake levels at  
 117 about 2300 cal BP followed by a significant drop in  
 118 lake level during the last millennium (Damnati et al.  
 119 2015).

120 Most of the paleoclimate and environmental recon-  
 121 structions in the Middle Atlas are based on fossil  
 122 pollen assemblages from lake sediments. These stud-  
 123 ies revealed a common pattern: the limited presence of  
 124 *Cedrus atlantica* Manetti pollen in the early Holocene,  
 125 with the general expansion of the species from the  
 126 Mid-Holocene which has been interpreted primarily as  
 127 evidence of increased moisture availability (Lamb

et al. 1989; Cheddadi et al. 1998, 2015, 2019; Rhoujjati et al. 2010; Nour El Bait et al. 2014; Tabel et al. 2016; Campbell et al. 2017). However, a recent study demonstrated a Mid-to Late Holocene summer aridity in the Middle Atlas using stable carbon isotope analysis of isolated fossil *Cedrus* pollen (Bell et al. 2019). Furthermore, several studies detected a Mid-Late Holocene aridification trend from ecological or hydrological records in the western Mediterranean (Jalut et al. 2009; Carrión et al. 2010; Jiménez-Moreno et al. 2015).

In order to strengthen paleolimnological interpretations inferred from a single proxy it is important to combine as many records as possible in a technique known as a multi-proxy approach (Bradley 2015). Some investigations have reconstructed lake paleohydrology in the Middle Atlas region using multi-proxy analysis of lacustrine terraces (Damnati et al. 2015) and of continuous sedimentary records (Nour El Bait et al. 2014; Zielhofer et al. 2017). For example, in Aguelmam Sidi Ali, Zielhofer et al. (2017) reconstructed the Western Mediterranean hydro-climatic variability, seasonality and forcing mechanisms during the last 12,000 year using a multi-proxy approach based on magnetic susceptibility, carbonate and total organic carbon content, core-scanning and quantitative XRF, stable isotopes of ostracod shells, charcoal counts, *Cedrus* pollen abundance, and diatom data. Only a few records span the Late Holocene period and more investigations and a regional review of the available lake records are needed. This would enable details of the contrasting spatial and temporal hydrodynamics of Middle Atlas lakes in response to climate-related variability to be verified.

Here we present continuous and high-resolution records of a sedimentary sequence recovered from “Flowers Marsh” (unofficial name), a karstic waterbody in the SW Middle Atlas, northern Morocco. The approach is based on radiometric techniques for dating, sediment geochemistry using XRF, sediment mineralogy using DRX, as well as biological indicators, including diatoms, coprophilous fungi spores, and ostracods. The overall aim of this paper is to provide a reconstruction of Flowers Marsh development in response to catchment changes and to regional climatic events during the Mid- to Late Holocene. Specifically, we will address the following questions: (1) what was the hydrological behavior of Flowers Marsh during the Mid- to Late Holocene? (2) Is there

any synchronicity and/or validation between the proxy records? (3) Are there any similarities with other regional climatic archives? (4) Is there any evidence for a Flowers Marsh response to variability of the Holocene climate at different scales?

#### Study site

The Middle Atlas is an intracontinental mountain chain in northern Morocco (Fig. 1a). It exhibits a large synclinal trough extending 250 km with a SW–NE trend. The geology of the region ranges from Palaeozoic to Quaternary and is dominated mainly by Triassic red beds covered by karstified Liassic limestones and dolomites, Palaeozoic sandstone, schist, quartzite and doleritic basalt (Martin 1981). The geomorphology and structural features of the region favor the formation of natural permanent or seasonal lakes. The genesis of these wetlands is a product of subsidence related to an intense fault network and karstification of dolomites (Hinaje and Ait Brahim 2002). The climate in the region is a mountain Mediterranean type with sub-humid to cold winters. The mean annual precipitation in the area approaches 900 mm year<sup>-1</sup>, mostly occurring between October and April (Martin 1981) and the average monthly temperature varies between - 2 °C and 31 °C (Chillassé et al. 2001). Evergreen oak (*Quercus rotundifolia*) and Atlantic cedar (*Cedrus atlantica*) are the main forest vegetation (Flower et al. 1989).

The studied site, Flowers Marsh (32°59'04''N, 5°27'13''W), is a small pond lying about 1554 m above sea level (asl) in the Middle Atlas Mountains, in the High Oum Er-rbia catchment (Fig. 1a). The waterbody's name comes from the floating hydrophytes that cover the water surface. The surface area of Flowers Marsh varies between 6 and 12 ha depending on the season. During wet climatic periods and high aquifer phases, water levels in Flowers Marsh may be controlled through sub-surface inflows and/or through local rainfall. During low stands, this pond is mainly controlled by the surface runoff. Flowers Marsh is located near Aguelmam (Fig. 1d), one of the largest lakes in the Middle Atlas region (55 ha). Aguelmam Azigza and Flowers Marsh belong to the same basin with a catchment area of 1020 ha (Jouve et al. 2019). Hydrological results from Aguelmam Azigza reveal that lake levels were closely linked to subsurface circulation with a high sensitivity to climate

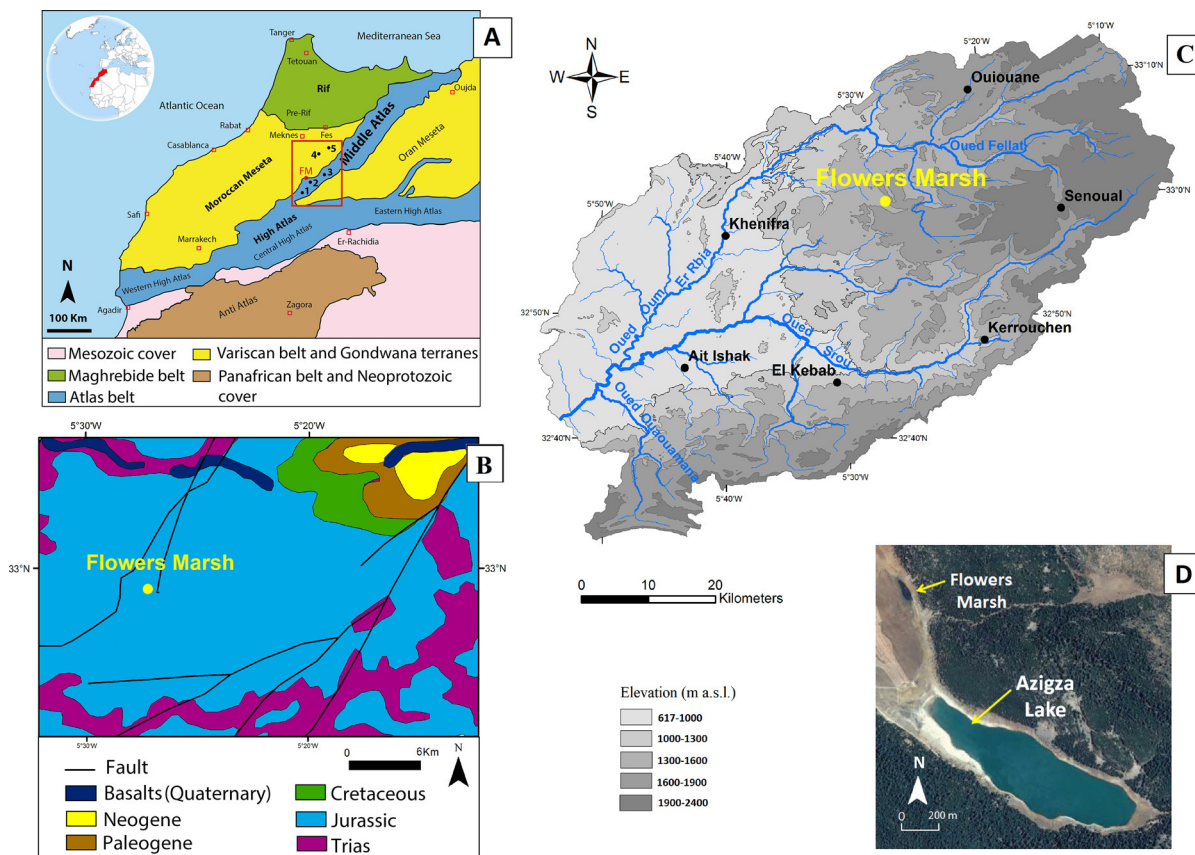


**Fig. 1** Location of the studied area. A: Simplified map showing the major geological provinces of Morocco. (modified from Saadi 1982) and the location of the study site (FM) and other paleoclimate studies cited in the text: 1, Ait Ichou Marsh (Tabel et al. 2016); 2, Lake Tigalmamine (Cheddadi et al. 1998; Lamb and van der Kaars 1995; Lamb and van der Kaars 1995; Cheddadi et al. 1998); 3, Aguelmam Sidi Ali (Campbell et al.

2017; Zielhofer et al. 2017); 4, Ras El Ma marsh (Nour El Bait et al. 2014); 5, Lake Iffer (Damnati et al. 2015). B: Simplified geological map of Morocco 1/1 000 000. C: Map of the High Oum Er-Rbia watershed, including topography and hydrographic network. D: Satellite image (Google Earth-2016) showing Flowers Marsh and Aguelmam Azigza situation

224 fluctuations especially precipitation (Vidal et al. 2016;  
 225 Adalall et al. 2019). From observations of paleoshore-  
 226 lines in the catchment (Flower and Foster 1992) and  
 227 past hydrological reconstructions (Jouve et al. 2019),  
 228 previous studies inferred that significant variations  
 229 have occurred in the level of Aguelmam Azigza. High  
 230 resolution Digital Elevation Models (DEM) from  
 231 Aguelmam Azigza watershed indicate that lake levels  
 232 need to be 10–15 m above modern levels for the two  
 233 waterbodies to be connected. Arial photographs from  
 234 1964 suggest that this connection has happened in the  
 235 past (Jouve et al. 2019).  
 236

**Materials and methods**

237

The studied cores were recovered in 2016 from  
 238 Flowers Marsh using a 50-cm-long Russian corer.  
 239 Two lake-marginal cores were taken: AZA-SUP-1-A-  
 240 16 and AZA-SUP-1-16. The length of each sequence  
 241 is 300 cm and 250 cm, respectively. Sediment core  
 242 stratigraphy was described on-site. The core segments  
 243 were wrapped in Clingfilm and stored in a cold storage  
 244 room at 4 °C. The two cores show a good visual  
 245 agreement and a very similar lithologic and chemical  
 246 succession (ESM1). Only the long core AZA-SUP-1-  
 247 A-16 was selected for this study.  
 248

In total, 21 subsamples were recovered at 15-cm  
 249 intervals for particle size analysis. Subsammles were  
 250

analyzed using a Horiba LA-300 laser diffraction analyzer at the Georesources Laboratory (Marrakech, Morocco). Subsamples were not pretreated before analysis and measurements were made on the fine sediment fraction (< 0.5 mm). The abundance of three grain size fractions was determined: clays (< 2 μm), silts (2–67 μm) and sand (> 67 μm).

To examine variations in sediment geochemistry, high-resolution X-ray fluorescence (XRF) was undertaken on the fresh core using an Itrax core-scanner (Cox Analytical Systems) at CEREGE (Centre de Recherche et d'Enseignement en Géosciences de l'Environnement), Aix-en-Provence, France. Sediment was analyzed with 500 μm spatial resolution and a molybdenum (Mo) tube at 30 kV, 40 mA and 15 s per interval analyzed. Relative abundance of elements (Fe, Ti, Mn, Si, K, Ca, Sr and Br) as well as incoherent and coherent X-ray backscatter were determined for the sedimentary sequence. Here we use the ratio of incoherent to coherent X-ray scatter (inc/coh) as a proxy for organic matter content in lake sediments, according to Brown et al. (2007). Elemental XRF intensity can be related to processes taking place within the lake. Titanium, K, Fe and Si can represent terrigenous sediment input linked to erosional parameters (Croudace et al. 2006; Olsen et al. 2012). In this research, K intensity is interpreted to reflect variations in detrital input (Aufgebauer et al. 2012). The Ca/Ti ratio mainly reflects Ca derived from within-lake processes and can be used to identify the occurrence of endogenic carbonate concretions in the sediments (Brown et al. 2007). Bromine (Br) has been regarded as a potential proxy for identifying relative variations in organic content in lake sediments (Kalugin et al. 2007; Gilfedder et al. 2011) and the Br/Ti ratio is an important proxy for productivity (Agnihotri et al. 2008). Manganese (Mn) contents may be related to changing redox conditions at the water-sediment interface in the lake (Davies et al. 2015) with high Mn content reflecting oxygenation of bottom waters (Kylander et al. 2011). Strontium (Sr) reflects aragonitic and evaporitic concretions (Arz et al. 2003).

The total carbon (TC%) and total organic carbon (TOC%) contents were determined for ten samples from the AZA-SUP-1-A-16 core with a FlashSmart NC Soil Thermo elemental analyzer at CEREGE. The standard deviation for standard carbonate materials was 0.07%, and the relative error of replicates was < 2.29%. The TOC was measured following standard

procedures after acidification (to eliminate the carbonate fraction). Total inorganic carbon (TIC) was determined using the following equation (Espitalié et al. 1977):

$$\text{CaCO}_3(\%) = (\text{TC} - \text{TOC}) \times 8.33$$

Mineralogical composition was examined from bulk sediments for selected representative samples by X-ray diffraction (XRD) with a SmartLab SE at CAC (Centre d'Analyse et de Caractérisation), Marrakech. Relative mineral abundance was determined using peak intensity with PANalytical X'Pert HighScore Plus software. The main minerals occurring are expressed as percentages.

The microstructures and element content of endogenic carbonates were determined using a scanning electron microscope (SEM) equipped with an energy dispersive spectrometer (EDS) at the CAC. The microscope was operated at 10 kV with a magnification of 116. The SEM and EDS allow the acquisition of photographs and elemental content.

Stable isotope analyses were carried out on fossil ostracods retrieved from Flowers Marsh sediments. Core AZA-SUP-1-A-16 was sampled at 1 cm intervals. The samples were sieved through a 63 μm mesh under tap water. Ostracods were only present in the upper 166 cm of the core and were handpicked from each sediment subsample using a binocular microscope and washed in deionized water. Carbon and oxygen isotopic analyses were performed on the two most abundant species separately: *Candona neglecta* and *Illyocypris gibba*. Adult ostracod shell material from *C. neglecta* species was used for C and O stable isotope analyses. In addition, stable isotopes were analyzed on the total dissolved inorganic carbon (TDIC) of Aguelmam Azigza water (lake and spring) and on modern ostracods (*C. neglecta* and *I. gibba*). The isotopic composition of endogenic carbonates extracted from the bulk sediment of the Flowers Marsh sequence was also analyzed. Measurements were performed using a Finnigan Delta Advantage mass spectrometer coupled to a Kiel III Device at CEREGE. The isotopic results were reported relative to the Vienna Pee Dee Belemnite (VPDB) standard. Analytical precision of δ<sup>18</sup>O and δ<sup>13</sup>C was 0.07‰ and 0.05‰, respectively.

The AZA-SUP-1-A-16 core was subsampled for diatom analysis at CEREGE. Sediment samples were prepared for smear slide analysis to determine the

348 presence of diatoms. Only 9 samples contained  
349 abundant diatoms. Wet sediment samples were treated  
350 using H<sub>2</sub>O<sub>2</sub> (33%) and HCl (10%) in order to remove  
351 organic matter and carbonates respectively. Slides  
352 were mounted in Naphrax and observed with an  
353 optical microscope (Nikon 80i 1000 × magnification  
354 with Nomarski optics, n.a.= 1.32). Taxonomic iden-  
355 tification and assignment of planktonic and benthic  
356 habitats were based primarily on Krammer and Lange-  
357 Bertalot (1986–1991) and Marciniak (1986).

358 Eight samples throughout the core were examined  
359 for coprophilous fungal spore abundances and treated  
360 according to Fægri and Iversen (1989) at CEREGE.  
361 *Lycopodium clavatum* tablets were added to each  
362 sample allowing determination of spore concentra-  
363 tions (Stockmarr 1971). Coprophilous fungi spores  
364 were identified according to the van Geel classification  
365 (2002). Identification was limited to the most abundant  
366 species: *Delitschia*-type, *Sordaria*-type, *Tripteros-  
367 pora*-type, UG-1138-type and focusing on *Sporor-  
368 miella*-type. The latter is an ascomycete fungus used  
369 as a specific indicator of herbivore presence (Davis  
370 and Schafer 2006; Cugny et al. 2010). Results are  
371 expressed as concentrations (spores cm<sup>-3</sup>).

372 The chronology of the lake core was constrained by  
373 9 Accelerator Mass Spectrometry (AMS) radiocarbon  
374 analyses performed on organic bulk sediments at Beta  
375 Analytic Inc laboratory, Florida, USA. Over the  
376 300 cm sequence, the age-depth relationship was  
377 constructed by linear interpolation of calibrated  
378 radiocarbon dates using the classical age modeling  
379 code (CLAM) for the statistical software R developed  
380 by Blaauw (2010), which also performs the calibration  
381 (using the SHCal13.14C, Reimer et al. 2013).

382 Multivariate statistical analyses were applied to the  
383 high resolution XRF dataset in order to extract and  
384 assess elemental correlations downcore. First, to  
385 attenuate non-linear matrix effects and constant sum  
386 constraints, the multivariate statistical analysis was  
387 applied after centered log-ratio (clr) transformation  
388 (Aitchison 1982; Weltje et al. 2015) of the complete  
389 set of XRF measurements (n = 5684). This simple  
390 transformation provides a reliable basis for statistical  
391 analysis of XRF core scanning data, unlike element  
392 count intensities or element ratios (Weltje et al. 2015).  
393 The following elements were considered for statistical  
394 analysis: Si, K, Fe, Ca, Ti, Mn, Sr and inc/coh. The Br  
395 was excluded because it frequently presents null  
396 values and dealing with clr transformation excludes

397 dealing with zeros. The clr transformation was carried  
398 out using CoDaPack, a freely available Excel based  
399 software for compositional data transformation (Thió-  
400 Henestrosa and Martín-Fernández 2006). As a second  
401 step, a normality assumption test was first applied  
402 using the Shapiro–Wilk test (Ghasemi and Zahediasl  
403 2012) in order to determine the type of correlation  
404 analysis to be used. Spearman’s rank correlation  
405 coefficient was then performed as a non-parametric  
406 measure of correlation between the monitored vari-  
407 ables (King and Eckersley, 2019) in order to quantify  
408 the strength of correlation between elements within  
409 each lithological unit. The correlation matrix was  
410 visualized as a heatmap with a dendrogram calculated  
411 by hierarchical clustering analysis (HCA) using the  
412 “heatmap” function implemented in the R package  
413 corrplot (Wei et al. 2017). The “rcorr” function in the  
414 Hmisc package (Harrell et al. 2006) was used to  
415 compute the significance levels for the Spearman  
416 correlations. Correlations with a *p*-value < 0.05 were  
417 considered significant.

## 418 Results

### 419 Chronological model

420 The chronological model of the AZA-SUP-1-A-16  
421 core was established based on 9 AMS <sup>14</sup>C dates  
422 (Fig. 2, ESM2). Two dates were rejected (samples  
423 obtained at 27 cm and 75 cm) because they were  
424 much older than expected, likely due to reworking of  
425 older lake deposits. According to the resulting age  
426 model based on the remaining ages, the sedimentary  
427 sequence reveals a robust and coherent chronology,  
428 providing a continuous record for the last 6,000 years.  
429 The mean sedimentation rate is low, about 0.8 mm  
430 yr<sup>-1</sup>, and varies between 0.1 and 2 mm yr<sup>-1</sup> down  
431 core.

### 433 Lithology and mineralogical contents

434 Four sedimentary units were defined on the basis of  
435 variations in described sediment lithology and micro-  
436 scopic observation (Fig. 3). The basal A unit (bottom-  
437 180 cm) comprises massive minerogenic sediments  
438 with a compact, gray-to-light-reddish, clayey-silt  
439 facies with poor preservation of biologic indicators

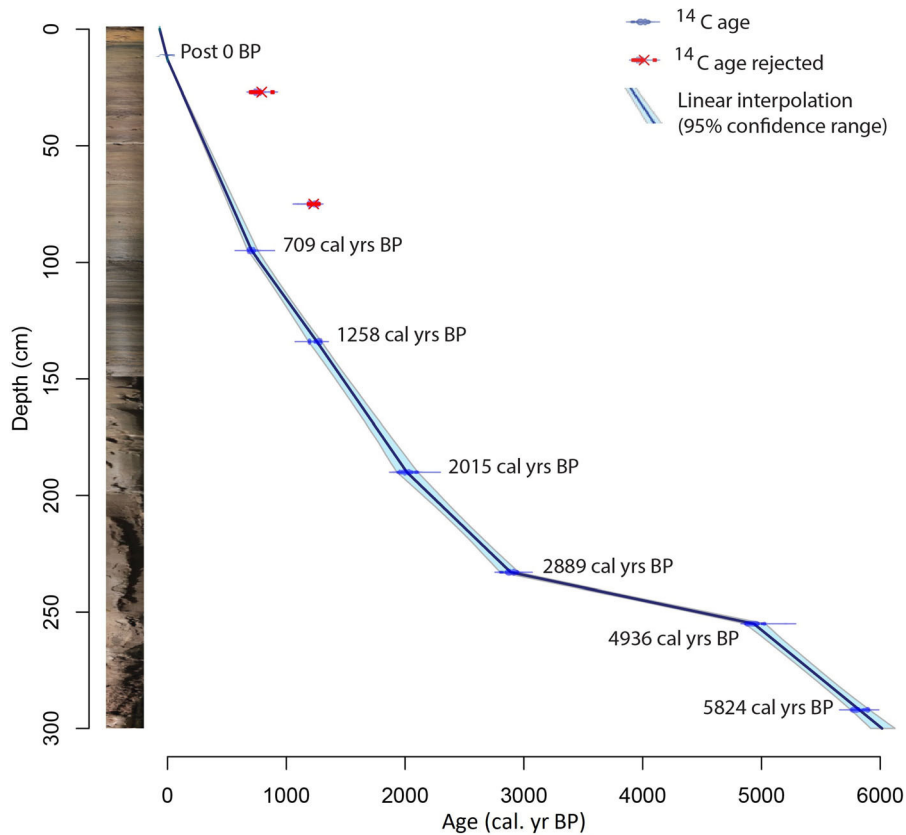


**Fig. 2** Chronological model of Flowers Marsh core (AZA-SUP-1-A-16) based on a linear interpolation of calibrated radiocarbon dates

440 and eroded pollen. The sediment of this unit has the  
 441 highest proportion of siliciclastic minerals (quartz,  
 442 phyllosilicates, goethite), and the lowest proportion of  
 443 calcite (Fig. 3). Unit B (between 180 and 150 cm)  
 444 represents a transitional interval between the predom-  
 445 inantly massive lower unit A and the upper laminated  
 446 unit C. This unit B is characterized by a high  
 447 proportion of siliciclastic minerals (quartz) and a  
 448 gradual increase in carbonate content (Fig. 3). It is  
 449 also characterized by well-preserved or fragmented  
 450 ostracod shells, gastropods and charophytes. Unit C  
 451 (150–90 cm) is formed of massive to faintly-lami-  
 452 nated, black to dark-gray, organic-rich facies with  
 453 abundant diatoms. It shows a marked up-core increase  
 454 in carbonate content. XRD results clearly indicate that  
 455 calcite is the dominant carbonate mineral (Fig. 3).  
 456 Finally, unit D (the upper 90 cm) is dominated by  
 457 laminated brown sediment. It is characterized by high  
 458 calcite content and the recurrence of ostracod shells.  
 459 Dark laminated facies with abundant diatoms, similar  
 460 to unit C facies, are observed in the upper part of this

unit (10–20 cm). Siderite and rhodochrosite, absent in  
 the lowermost units A and B, are present within units  
 C and D in low percentages (Fig. 3).

Grain size analysis of AZA-SUP-1-A-16 showed  
 that the sediments of Flowers Marsh consist predom-  
 inantly of clay and silts in the lower part of the core  
 (units A and B) while a sandy fraction dominates the  
 upper part of the core (units C and D; Fig. 3). This  
 sandy fraction results mainly from the presence of  
 endogenic carbonate concretions called “cauliflow-  
 ers” rather than from detrital sand from the watershed  
 area. “Cauliflowers” were only detected in units C and  
 D. The high endogenic carbonate content of units C  
 and D is in good agreement with the TIC and the  
 CaCO<sub>3</sub> content, underlining the strong carbonate  
 precipitation in the upper part of the core. High-  
 resolution images of these endogenic carbonates  
 obtained by SEM yielded observation of their  
 microstructures. The morphology of the calcite crys-  
 tals is irregular having “cauliflower” shapes and

461  
 462  
 463  
 464  
 465  
 466  
 467  
 468  
 469  
 470  
 471  
 472  
 473  
 474  
 475  
 476  
 477  
 478  
 479  
 480  
 481

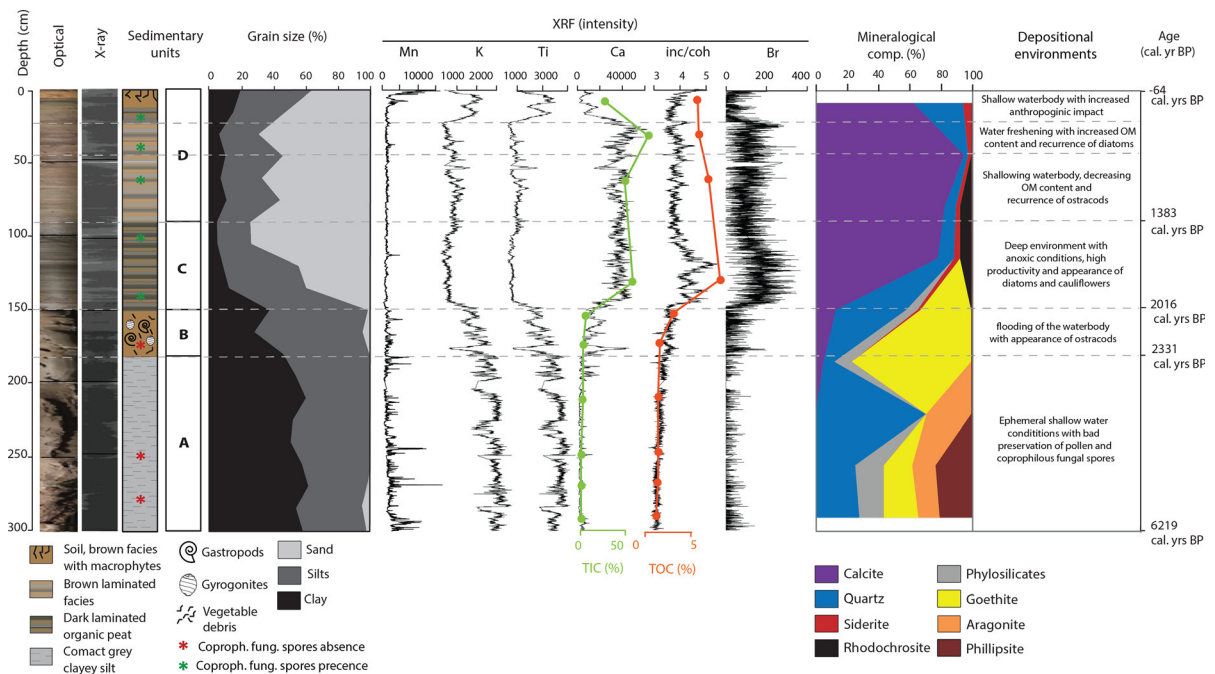


**Fig. 3** Physical and lithological properties of Flowers Marsh core sediment. From left to right: Core image, X-ray radiography, schematic lithology, sedimentary units, grain size distribution (clay, silt and sand), X-ray Fluorescence (XRF) core scanner data expressed as intensity (Mn, K, Ti), Ca-XRF and

Total Inorganic Carbon (TIC), inc/coh, Total Organic Carbon (TOC) and Br, mineralogical composition, reconstructed depositional environments and chronological scale (in cal. years BP)

482 shows a rough and porous surface and no obvious  
 483 internal structure (ESM3-A). The EDS analysis  
 484 showed that the elemental composition of this mineral  
 485 includes O, C and Ca and small amounts of Mg, K, and  
 486 Fe, indicating the calcic nature of these endogenic  
 487 carbonates (ESM3-B).

488 **Geochemistry**

489 *Elemental geochemistry*

490 The main chemical elements and ratios selected for  
 491 this study are the following: K, Si, Ti, Fe, Ca, Br,  
 492 inc/coh, Ca/Ti and Br/Ti. Downcore elemental profiles  
 493 are clearly consistent with the facies distribution  
 494 (Figs. 3 and 4, ESM4). Si, K, Ti and Fe show  
 495 comparatively higher values in clastic-dominated  
 496 intervals in unit A and reveal a decrease in unit B  
 497 with lower values in units C and D. The top of unit D  
 498 shows an increase in the elements. Calcium displays  
 499 an opposite trend, reaching maximum values in the  
 500 carbonate-rich facies of units C and D. The inc/coh  
 501 ratio and Br exhibit rather low and constant values in

units A and B, then present abrupt increases in  
 organic-rich intervals of unit C, decreasing upwards  
 (Fig. 3, ESM4). The Ca/Ti and Br/Ti ratios display  
 similar trends and present very low values in units A  
 and B and higher values within units C and D.  
 Manganese contents show a variable pattern with  
 higher peaks in unit A and B and in the uppermost  
 layer of unit D (Fig. 3).

Since changes in the core lithology reveal consid-  
 erable variation in the lake status, correlation analysis  
 and hierarchical clustering were constructed within  
 each unit to quantify the strength of correlation  
 between the lithology and geochemical composition  
 (Fig. 5). The main detrital elements (K, Ti, and Fe)  
 correlate strongly in all units ( $r = 0.58-0.96$ ,  $p$ -  
 value =  $< 0.0001$ ). Silicon shows good correlations  
 with the detrital elements in Unit A, B and D. This is  
 not the case in the diatoms-rich unit C, where Si  
 displays low correlations with these detrital elements.  
 The inc/coh ratio shows a strong correlation with Ca in  
 unit D ( $r = 0.84$ ;  $p$ value  $< 0.0001$ ;  $n = 1760$ ), a  
 moderate correlation in unit C ( $r = 0.61$ ;  
 $p$  value  $< 0.0001$ ;  $n = 1154$ ) and unit B ( $r = 0.58$ ; $p$ -

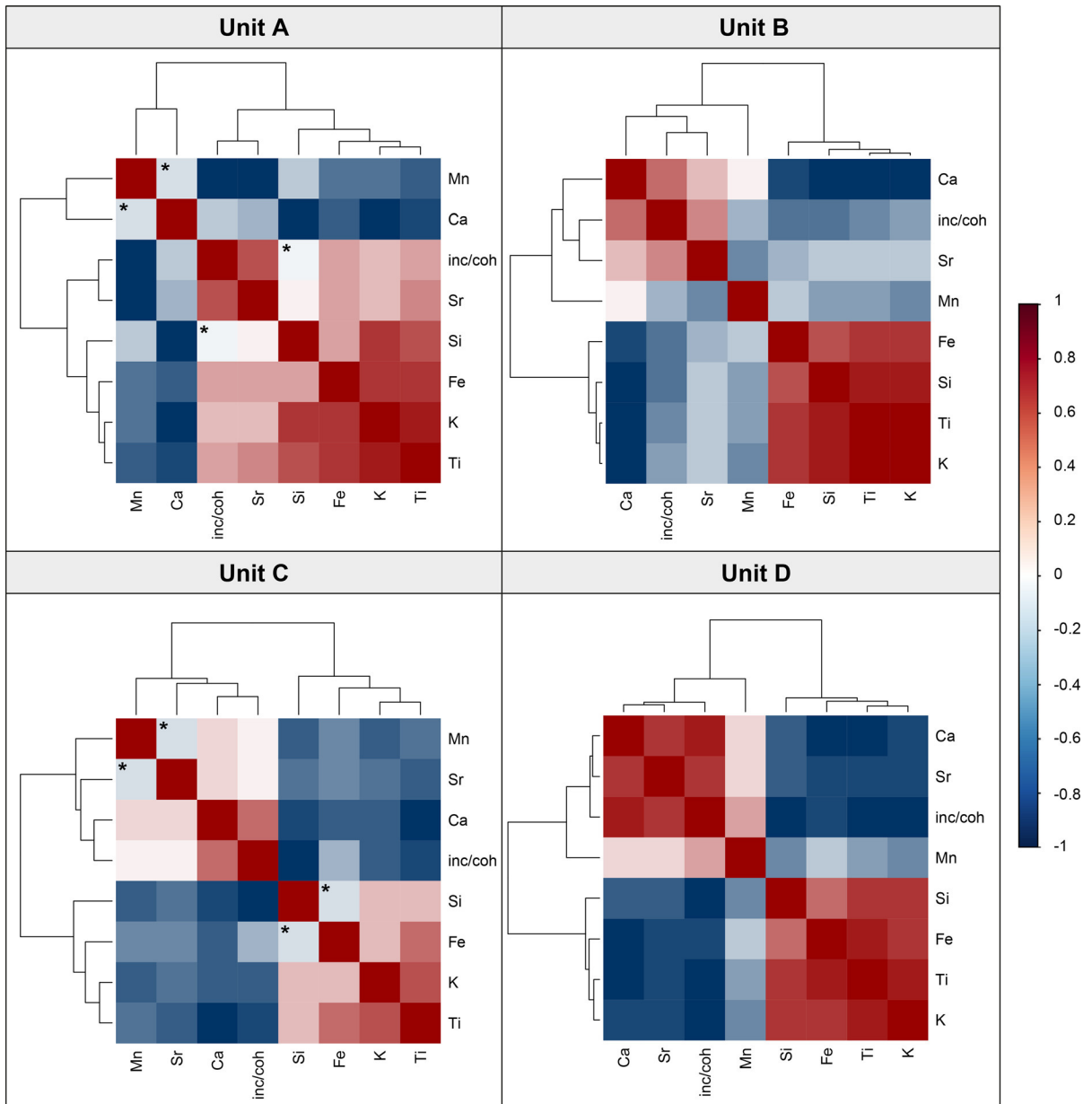


**Fig. 4** Spearman correlation matrix and hierarchical clustering of the main XRF elements for the four lithological units (A, B, C and D). Red colors indicate positive correlations and blue colors indicate negative correlations. The color gradient indicates the

strength of correlation. The order of the elements determines the ordered clusters. Asterisks refer to correlations with  $p$ -values  $> 0.05$ . Correlations without asterisks have a  $p$  value  $< 0.0001$  (ESM6)

525 value  $< 0.0001$ ;  $n = 600$ ) and a very low correlation  
 526 in unit A ( $r = -0.09$ ;  $p$ -value  $< 0.0001$ ;  $n = 2170$ ).  
 527 The Mn does not show any correlation with other  
 528 elements and likely reflects changes in redox condi-  
 529 tions. Generally, the HCA dendrogram shows two  
 530 clear main clusters: one associated with detrital

minerals (Ti, K, Fe and Si) and the second one linked  
 with organic matter and carbonate minerals (inc/coh,  
 Ca and Sr); these two groups are clearly negatively  
 correlated. In unit A, Sr and inc/coh show a weaker  
 connection to the detrital elements group. Manganese  
 is weakly related to the organic matter cluster.

531  
 532  
 533  
 534  
 535  
 536

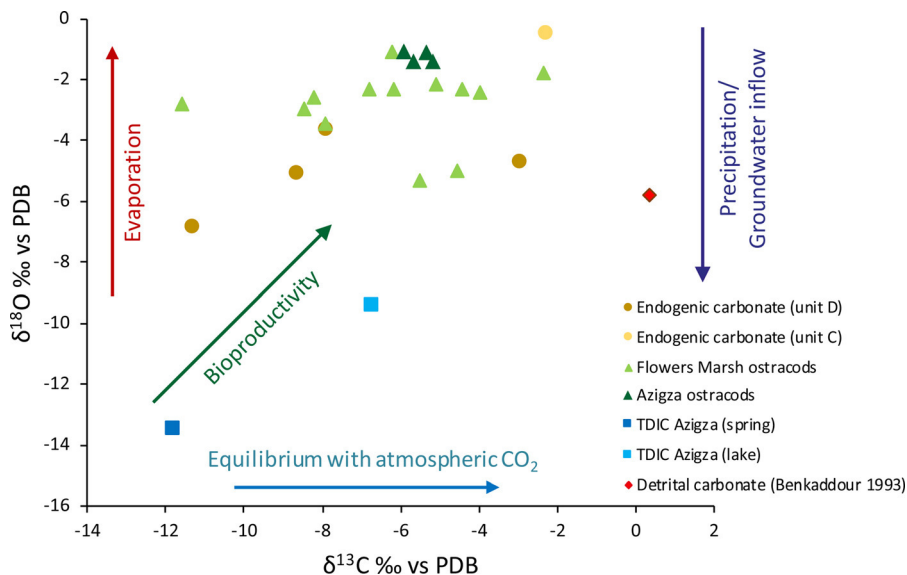


**Fig. 5** Crossplot of  $\delta^{13}\text{C}$  versus  $\delta^{18}\text{O}$  for the studied endogenic and biogenic carbonates (ostracods) from Flowers Marsh, modern ostracods and TDIC from Aguelmam Azigza and

published isotope composition of detrital carbonate obtained from the study area (Benkaddour 1993)

537

### 538 Organic geochemistry

539 The TOC values of the Flowers Marsh sequence range  
540 from 1% to 8% (Fig. 3). The organic content of units A  
541 and B is relatively low and constant (oscillating  
542 around 1%), increasing in the top of unit B (3.1%) and  
543 reaching maximum values of 8.3% in the lower part of  
544 unit C. The TOC remains relatively high in unit D  
545 (values range between 5 and 7%) with a decreasing  
546 trend towards the core top. The inc/coh ratio shows a  
547 similar trend to TOC, suggesting it is a reliable proxy  
548 for organic content in this system. Similarly, TIC  
549 values show a general trend towards increasing values  
550 from the bottom (unit A and B) to the top of the core  
551 (unit C and D). The highest concentrations of up to  
552 75% occur at 32 cm and the lowest (0.5%) at the base  
553 of the core.

### 554 Biological proxies

555 The occurrence of ostracod shells is limited to the  
556 upper 166 cm of the Flowers Marsh sequence (166–  
557 143 cm and 25–79 cm); no shells were found in units  
558 A and B. When ostracods were observed, *Candona*

*neglecta* and *Illyocypris gibba* were the most abundant  
559 species. 560

561 Diatom content is low throughout most of the  
562 record, and diatom remains are poorly 382 preserved.  
563 Diatoms present a sharp contrast with the abundance  
564 of ostracods. Units A and B were sterile in regards to  
565 diatoms. Unit C (150–90 cm) is dominated by  
566 epiphytic species such as *Epithemia adnata* (Kützing),  
567 *Sellaphora laevisissima* (Kützing) and *Gomphonema*  
568 *pumilum* (Grunow) and by benthic species represented  
569 mainly by *Halamphora veneta* (Kützing) and *Coc-*  
570 *coneis placentula* (Ehrenberg) (ESM5). In the upper  
571 90 cm, the diatom assemblage is still dominated by  
572 benthic forms, except at 47–48 and 38–39 cm where  
573 the centric *Cyclotella distinguenda* (Hustedt) domi-  
574 nates the assemblage (ESM5).

575 The occurrence of coprophilous fungi species and  
576 spore concentration throughout the core were exam-  
577 ined. The lowest units A and B (280, 250 and 174 cm)  
578 present low concentrations and poor preservation of  
579 coprophilous fungi spores. The boundary between  
580 units B and C (141 cm) is characterized by an increase  
581 in values of coprophilous fungi spores with a better  
582 preservation and high abundances of the UG-1138  
583 species. In unit C (101 cm), continuation of the high  
584 values of UG-1138 is recorded. The exclusive occur-  
585 rence and high values of *Tripterospora*-type and a

586	decrease in UG-1138 values occur in unit D (39 cm).	proposed in order to demonstrate the local hydrologi-	630
587	The topmost part of this unit (19 cm) is characterized	cal differences and the common patterns in response	631
588	by the highest values of <i>Sporormiella</i> -type and a	to regional climatic drivers.	632
589	relatively high abundance of <i>Delitschia</i> -type.		
590	$\delta^{13}\text{C}$ and $\delta^{18}\text{O}$ of Flowers Marsh carbonates	Flowers Marsh hydrological development	633
		during the last 6000 years	634
591	The oxygen isotopic composition values of biogenic	Four main phases were distinguished following the	635
592	carbonates derived from the benthic ostracod species	lithologic units, the geochemical zonation derived	636
593	<i>C. neglecta</i> were in the range $-5.34$ to $-1.09\%$ .	from the $\mu\text{-XRF}$ data, the mineralogy and the recur-	637
594	These values are in agreement with ostracod $\delta^{18}\text{O}$	rence of biomarkers (Fig. 4): (A) ephemeral water-	638
595	records measured on the same species in the larger	body, (B) flooding and permanent shallow water	639
596	lake Aguelmam Azigza (this study) and with records	conditions, (C) medium to deep waterbody and	640
597	carried out on modern ostracods from Lake Tigel-	(D) shallow water level.	641
598	mamine (Benkaddour et al. 2005). The $\delta^{18}\text{O}$ of		
599	ostracods is mostly affected by the isotopic composi-	<i>Unit A—Ephemeral waterbody (6–2.3 cal. kyr BP)</i>	642
600	tion of lake water and water temperature at the time of		
601	its formation (Xia et al. 1997). In semi-arid, closed	The oldest sediments present in the Flowers Marsh	643
602	small lake settings, ostracod $\delta^{18}\text{O}$ reflects primarily	sequence are characterized by a high intensity of Ti, K,	644
603	the local hydrologic balance (Roberts et al. 2008;	Si which are grouped together with Sr and Fe (Fig. 5).	645
604	Develle et al. 2010).	These detrital elemental intensities may mostly track	646
605	Figure 6 displays the relationship between $\delta^{13}\text{C}$ and	high clay and phyllosilicate contents that are deposited	647
606	$\delta^{18}\text{O}$ for all of the carbonate species analyzed in this	during heavy rainfall and thus be related to a relatively	648
607	study. The $\delta^{13}\text{C}$ in the studied samples of endogenic	high lake level, or they may correspond to evidence of	649
608	carbonates from Flowers Marsh sediments vary consid-	arid conditions and thus be related to lake desiccation.	650
609	erably and range from $-11.3$ to $-2.3\%$ VPDB,	However, the highly clastic nature of unit A made up	651
610	whereas $\delta^{18}\text{O}$ of the same samples range from $-6.8$ to	of clay minerals, phyllosilicates and quartz particles	652
611	$-0.5\%$ VPDB. The dominant controls on the $\delta^{18}\text{O}$ of	(as determined by XRD and microscope observations)	653
612	lacustrine endogenic carbonates is controlled are the	with a very low sedimentation rate suggests that the	654
613	temperature of its formation and the isotopic composi-	sediments were originally deposited in a shallow,	655
614	tion of the water in which it precipitates (Epstein	littoral lacustrine setting. Furthermore, the minimum	656
615	et al. 1953; Craig 1965). The $^{13}\text{C}$ content of lacustrine	carbonate values (TIC, DRX calcite and Ca intensi-	657
616	carbonates mainly reflects the composition of the	ties) point to an absence of dissolved calcite from	658
617	TDIC in the lake water and the effects of biological	surrounding rocks, as a consequence of $\text{CO}_2$ -poor	659
618	fractionation related to aquatic photosynthesis (Stu-	groundwater associated with weakly developed soil	660
619	iver 1970; McKenzie 1985).	and vegetation and/or to low detrital carbonate input as	661
		a consequence of decreased runoff. The complete	662
620	<b>Discussion</b>	absence of biological fauna with non-preservation of	663
		coprophilous fungi spores and eroded pollen also	664
621	Paleoenvironmental interpretation of the deposited	supports oxic conditions typical of a shallow environ-	665
622	sediments requires an accurate understanding of the	ment with frequent periods of subaerial exposure	666
623	proxy significance. In the following, different proxies	(González-Sampéris et al. 2008). The low accumula-	667
624	are discussed to provide a reliable paleohydrological	tion of organic matter (extremely low TOC content)	668
625	reconstruction of Flowers Marsh. A possible connec-	may indicate a barren landscape with sparse vegeta-	669
626	tion with Aguelmam Azigza hydrological behavior is	tion and low productivity in the waterbody (low Br/	670
627	discussed so as to understand the hydrological func-	Ti). The absence of endogenic calcite (low Ca/Ti)	671
628	tioning of these hydrosystems at the catchment scale.	indicates that conditions were not adequate for endo-	672
629	Finally, comparisons between the regional records are	genic calcite precipitation and/or preservation in the	673
		sediments. In addition, the relatively high Mn contents	674

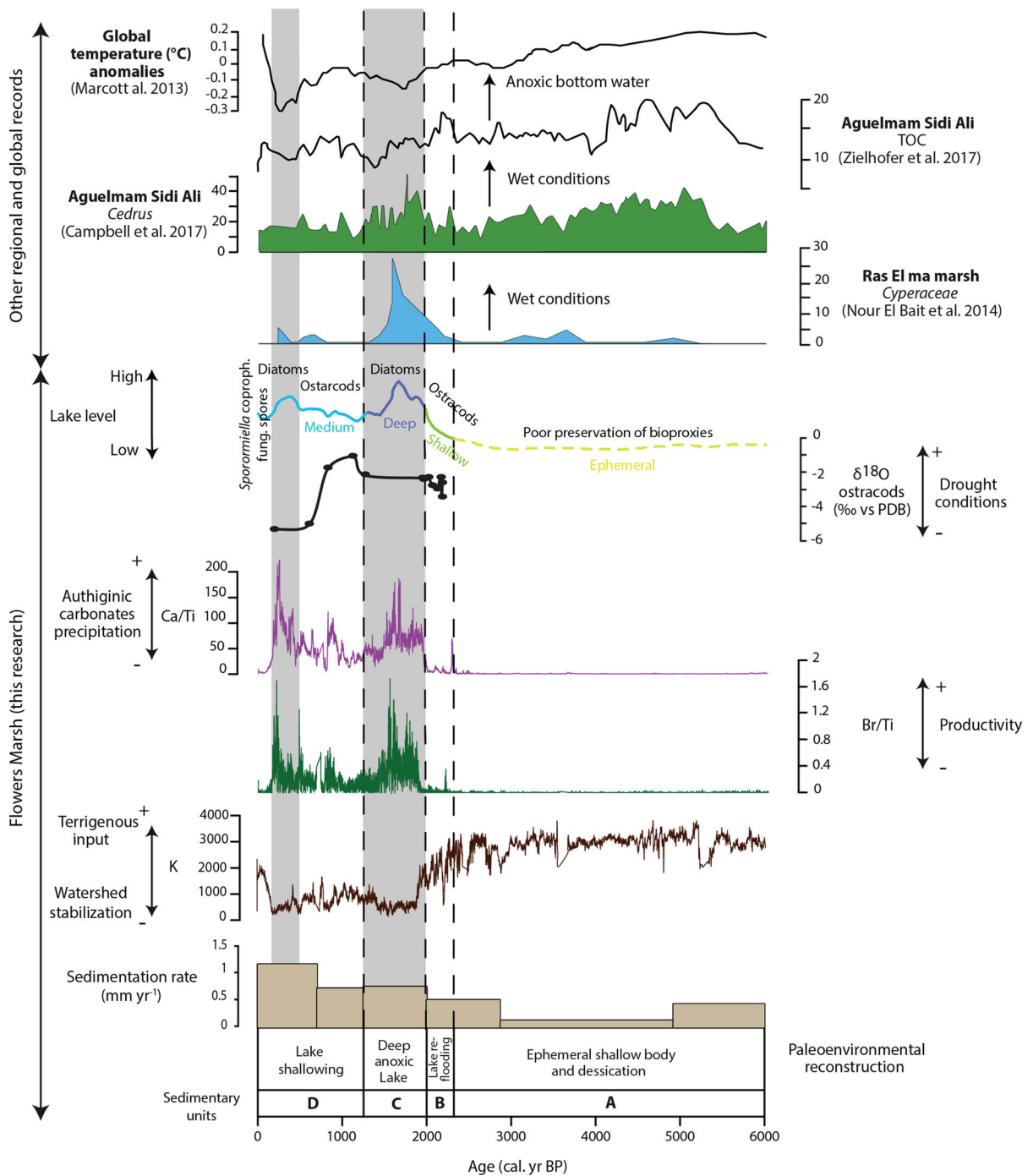


**Fig. 6** Selected Flowers Marsh proxies (lower part) compared with other regional and global records (upper part) for the last 6 cal. kyr BP. In the lower section, from bottom to top: calibrated radiocarbon dates, paleoenvironmental reconstruction for the different units (A-B-C-D), sedimentation rate (mm yr<sup>-1</sup>), K-XRF, Ca/Ti ratio, Br/Ti ratio, δ<sup>18</sup>O record from *C. neglecta* and the relative lake-level curve construction using different proxies mentioned in the text. In the upper section:

El Ma Marsh aquatic plant records (Nour El Bait et al. 2014), Aguelmam Sidi Ali *Cedrus* records (Campbell et al. 2017), TOC records (Zielhofer et al. 2017) and reconstruction of Global Temperature anomalies at the uppermost part of the record (Marcott et al. 2013). Vertical dotted lines represent temporal subdivisions of units used in the “Discussion” section. Grey shading highlights periods of high stand of Flowers Marsh

675 indicate oxygenation of the bottom sediment with  
676 increasing preservation of Mn as oxides (Davies et al.  
677 2015). Sedimentological, geochemical and biological  
678 evidence from unit A sediments indicates hydrological  
679 scenarios that fluctuate between a very shallow and an  
680 ephemeral waterbody. This interpretation is consistent  
681 with results from other lake sediments with no organic  
682 matter content and a high clastic content that were  
683 related to periods of shallow lake levels (Valero-  
684 Garcés et al. 2000; González-Sampériz et al. 2008;  
685 Corella et al. 2011; Nour El Bait et al. 2014).

686 *Unit B—re-flooding and shallow water conditions*  
687 *(2.3–2 cal. yr BP)*

688 Unit B is a transitional phase between the clastic  
689 material of Unit A and the laminated organic-rich  
690 sediment of the top of the core. It represents a  
691 progressive transition towards a shallow wetland  
692 environment with calcite formation marked by peaks  
693 in Ca/Ti. The high sedimentation rate underlines the  
694 increase in carbonate deposition (Fig. 4). This phase is  
695 characterized by the appearance of ostracods, espe-  
696 cially benthic species (*C. neglecta* and *I. gibba*). Their  
697 high abundance indicates that the lake-bottom condi-  
698 tions were predominantly aerobic during this interval  
699 (Meisch 2000). The abundance of charophytes and  
700 gastropods also indicates a shallower littoral environ-  
701 ment (Benkaddour 1993; Soulié-Märsche et al. 2008).  
702 The decline of terrigenous element contents can be  
703 explained by the stability of the watershed as  
704 confirmed by the forest cover expansion during this  
705 period (Lamb et al. 1999; Nour El Bait et al. 2014).  
706 Unit B deposits characterize the re-flooding of the  
707 waterbody marked by changes in the depositional  
708 mode which most likely resulted from climate ame-  
709 lioration in the region. Slight fluctuations of ostracod  
710  $\delta^{18}\text{O}$  values in this unit probably point to a shallow and  
711 steady water level (Fig. 4).

712 *Unit C—Medium to deep waterbody (2–1.4 cal. kyr*  
713 *BP)*

714 This unit was deposited under relatively deep water  
715 conditions as indicated by the preservation of lamina-  
716 tion, the highest TOC values (up to 8%) and diatom-  
717 and organic matter-rich facies, indicative of high  
718 biological productivity and organic matter preserva-  
719 tion in the lake (Martín-Puertas et al. 2011). The low

Mn content and the well preservation of pollen and  
spores point to deposition in a relatively anoxic deep  
lake (Brauer 2004; Zolitschka 2007; Martín-Puertas  
et al. 2009). This unit is characterized by a major  
change in grain size distribution from clay-silt to sand  
as the dominant particle sizes, associated with an  
increase in sedimentation rate (Figs. 3 and 4). This  
sandy fraction is related to the massive endogenic  
carbonate precipitation indicated by peaks in Ca/Ti  
(Fig. 4). These carbonate concretions are related to the  
occurrence of “cauliflowers” irregularly shaped car-  
bonate concretions that have been described as being  
of algal origin (Magny 1992). They reflect deposition  
in a shallow-water environment with mobilization to  
the deep basin during periods of higher runoff. In this  
unit, endogenic carbonates record the highest isotopic  
values (Fig. 6). Enriched isotopic values relative to the  
TDIC values may be related to high productivity  
(diatom and algal) in the littoral zone (Stuiver 1970;  
McKenzie 1985). The absence of ostracods during this  
interval is not due to calcite dissolution processes, as  
indicated by the presence of endogenic calcite. Most  
likely, diatom blooms, anoxic conditions and limited  
water circulation in the lake bottom as indicated by  
laminated sediments inhibited the survival of benthic  
ostracods (Valero-Garcés 2003). This unit is also  
characterized by negative shifts in Ti, K, Fe and Si  
indicators for allochthonous detrital input (Fig. 3,  
ESM4). This decrease could be related to the stability  
of the watershed by forest development and to dilution  
of the allochthonous input by precipitated calcite as  
indicated by the negative correlations of Ca with the  
detrital elements in unit C (Fig. 5). Silicon shows a  
low correlation with the detrital elements in this unit  
(Fig. 5), which highlights an additional source (bio-  
genic) of Si provided by diatoms.

*Unit D—Fluctuating and shallow pond (After 1.4 cal.*  
*kyr BP)*

758 During this period, Flowers Marsh sediments reflect  
759 the change from dark laminations (unit C) to brown-  
760 white laminations and several productivity proxies  
761 point to a slight decrease (TOC, inc/coh, Br/Ti and  
762 diatom abundance). A minor drop in carbonate  
763 precipitation also occurred, extending until  
764 ~ 650 cal. yr BP. This decline in primary productiv-  
765 ity and carbonate production together with more  
766 positive ostracod  $\delta^{18}\text{O}$  values, compared to the onset

767 of unit C, could be related to more arid conditions  
 768 (Fig. 4). Also, the replacement of diatoms by ostra-  
 769 cods points to a major shift in the lake level toward  
 770 shallow waters (Benkaddour 1993). A transitory  
 771 increase in the deposition of organic matter (high Br/  
 772 Ti) and calcite precipitation (high Ca/Ti) between 650  
 773 and 150 cal. yr BP points to a period of enhanced  
 774 biological productivity that allowed the precipitation  
 775 and preservation of endogenic calcite concretions  
 776 (Fig. 4). The diatom record is dominated by *Cyclotella*  
 777 *distinguenda* which indicates an enhanced lake level  
 778 and the dominance of a period of stable stratification  
 779 (Interlandi and Kilham 2001). A drop in ostracod  $\delta^{18}\text{O}$   
 780 values may reflect a short phase of more humid  
 781 conditions during this period (Fig. 4). Since 150 cal.  
 782 yr BP, another phase characterized by indicators of  
 783 lower productivity (decreases in TOC, inc/coh and Br/  
 784 Ti ratio) and increases in clastic input to the lake  
 785 occurred (Fig. 3). Stronger reduction of the waterbody  
 786 prevailed during this period as revealed by the high  
 787 Mn content indicating oxygenation of the lake bottom.  
 788 More arid conditions leading to enhanced littoral  
 789 erosion and sediment delivery to the pond may explain  
 790 the increase in detrital element contents. Nevertheless,  
 791 these trends could also be related to the anthropogenic  
 792 degradation of the landscape by increased farming or  
 793 land use practices including high pastoralism activi-  
 794 ties. An anthropogenic effect is supported by the  
 795 presence of anthropogenic markers such as the high  
 796 concentrations of *Sporormiella* (Cugny et al. 2010;  
 797 Williams et al. 2011; Currás et al. 2012) in recent  
 798 sediments (recorded at 180 cal. yr BP). This reflects an  
 799 increase in livestock grazing activity which is the main  
 800 anthropogenic pressure on soils in the area (Campbell  
 801 et al. 2017). Given the low temporal resolution of this  
 802 part of the core, the sub-millennial variability should  
 803 be interpreted cautiously in this part of the record.

#### 804 *Connection between Flowers Marsh and Aguelmam* 805 *Azigza*

806 The Flowers Marsh paleohydrological reconstruction  
 807 reveals interesting links to Aguelmam Azigza. The  
 808 flooding at 2.3 cal. kyr BP may be interpreted as a  
 809 period of enhanced surface and groundwater flux to  
 810 the pond. Earlier and recent studies from the nearby  
 811 Aguelmam Azigza indicate metric water level fluctu-  
 812 ations at interannual and decadal scales (Flower et al.  
 813 1989; Adalall et al. 2019; Jouve et al. 2019). Precise

geomorphological mapping of the watershed shows  
 that a connection existed between the two waterbodies  
 owing to a lake level increase at Azigza of about 15  
 meters, a level that was also reached in the late 1960s  
 (Jouve et al. 2019). We suggest that the re-flooding  
 period evidenced at the Flowers Marsh could corre-  
 spond to an equivalent Azigza lake-level high stand at  
 about 2.3 kyr BP. This would imply that the highest  
 Azigza lake level was probably reached at that time.  
 Precise geomorphological observations of the basin  
 catchments are consistent with a past high stand  
 (Jouve et al. 2019).

#### Comparison with Mid-Late Holocene regional records

In Europe and in the Mediterranean region, the  
 Holocene period reveals diverse spatial and temporal  
 patterns of climate variability induced by large-scale  
 changes in atmospheric circulation and complex  
 interactions of various forcing factors (Di Rita et al.  
 2018). The linkage between phases of aridity and  
 humidity on a sub-regional to regional scale is highly  
 challenging (Carrión 2002). The Moroccan Middle  
 Atlas is part of this Mediterranean periphery and has  
 also demonstrated local and regional sensitivity in the  
 response of lakes to climatic variation.

During the Mid-Holocene (6000–2300 cal. yr BP),  
 Flowers Marsh records ephemeral water conditions  
 with recurrent desiccation periods. This picture con-  
 trasts with evidence of a moister climate recorded in  
 the Middle Atlas region. Humid conditions were  
 highlighted by the arrival and expansion of cedar after  
 ~ 6 cal. kyr BP, recorded in Aguelmam Sidi Ali  
 (Campbell et al. 2017), Lake Tigalmamine (Lamb  
 et al. 1999), the Ras El Ma marsh (Nour El Bait et al.  
 2014), and the Ait Ichou marsh (Tabel et al. 2016).  
 This Mid-Holocene expansion of *Cedrus* was related  
 to increasing available moisture and suggests a  
 climatic transition toward generally cooler and more  
 humid conditions with reduced summer drought  
 (Campbell et al. 2017). However, other Middle Atlas  
 paleohydrological studies have detected a striking  
 mismatch between the local hydrological water bal-  
 ance and plant available moisture reflected by the  
 abundance of *Cedrus* pollen. For instance, a maximum  
 in plant available moisture recorded at Lake Tigal-  
 mamine coincides with low lake levels (Lamb and van  
 der Kaars 1995). Equally, the *Cedrus* pollen in the

861 Aguelmam Sidi Ali record indicates more humid  
 862 conditions during the Late Holocene, while the  
 863 majority of the lake level proxies point to a general  
 864 lake level lowering trend during this period (Zielhofer  
 865 et al. 2017). The authors interpreted *Cedrus* pollen  
 866 increases not as an indicator of more precipitation but  
 867 rather as an indicator for more available moisture that  
 868 may be the result of lower summer temperatures  
 869 (Lamb et al. 1999; Zielhofer et al. 2017). The low lake  
 870 level recorded in Flowers Marsh sediments during the  
 871 Mid- to Late Holocene may be related to a reduction in  
 872 winter precipitation which would have significantly  
 873 reduced groundwater recharge. During the Mid-  
 874 Holocene, arid conditions were recorded in lake  
 875 sediments in the Middle Atlas region (Rhoujjati  
 876 et al. 2012; Campbell et al. 2017; Bell et al. 2019),  
 877 and also in more distant sites from the northern Iberian  
 878 Peninsula (Santos et al. 2000; Morellón et al. 2008).  
 879 For instance, most of the saline lakes in the Central  
 880 Ebro valley (northeastern Spain) were desiccated or  
 881 ephemeral during the Mid-Holocene (González-Sam-  
 882 périz et al. 2008). In Arreo Lake, the presence of  
 883 coarse alluvial facies at the base of the sequence points  
 884 to more arid conditions prior to 2250 BP (Corella et al.  
 885 2013).

886 The Late Holocene is characterized by a transi-  
 887 tional phase towards a sustainable water supply to the  
 888 pond with a higher water level at Flowers Marsh  
 889 (2300 cal. yr BP–1800 cal. yr BP), particularly evi-  
 890 dent in lamination preservation and in organic matter  
 891 increase. Wet conditions during this period were also  
 892 recorded in Lake Iffer as indicated by an increase in  
 893 lake productivity and rising lake level (Damnati et al.  
 894 2015). At Tigalmamine Lake, increased precipitation  
 895 at about 2600 year BP, with equivalent troughs in  
 896 winter and summer temperatures were reconstructed  
 897 from pollen records (Cheddadi et al. 1998). Higher  
 898 lake levels are documented by the dominance of  
 899 aquatic plants (*Typha* L., *Potamogeton* Linn., *Myrio-  
 900 phyllum* L. and Cyperaceae) in the pollen diagram  
 901 from Ras El Ma marsh, with a high stand between  
 902 2000 and 1400 cal. yr BP (Fig. 4) (Nour El Bait et al.  
 903 2014). A relative increase in TOC around 2,200 cal. yr  
 904 BP was also recorded in Aguelmam Sidi Ali indicating  
 905 a high lake level and high productivity (Zielhofer et al.  
 906 2017). This period coincides with the wetter Iberian  
 907 Roman period in the northern Mediterranean. A humid  
 908 phase during the Iron Age and the Roman Optimum  
 909 from 2700 to 1600 year, inferred from lake and fluvial

910 records (Macklin et al. 2006; Martín-Puertas et al. 910  
 911 2008), has been found in the Iberian Peninsula. 911  
 912 Furthermore, a decrease in temperature around 912  
 913 2000 cal. yr BP was identified at a global scale 913  
 914 (Marcott et al. 2013). 914

915 The shallowing water level recorded at Flowers 915  
 916 Marsh since 1.4 kyr cal. BP coincides with decreasing 916  
 917 tree pollen abundance at other regional Lakes, such as 917  
 918 Aguelmam Sidi Ali where there was a reduction in the 918  
 919 arboreal/non-arboreal pollen ratio (AP/NAP) after 919  
 920 1300 cal. yr BP (Cambell et al. 2017). Most of the 920  
 921 Middle Atlas records reflect forest cover degradation 921  
 922 during this period, which might be related to more arid 922  
 923 conditions. This stage coincides with the Medieval 923  
 924 Climate Anomaly (MCA) which was marked by a 924  
 925 global increase in temperature (Marcott et al. 2013). It 925  
 926 has also been described in previous paleoclimatic 926  
 927 reconstructions across the Mediterranean Basin 927  
 928 (Magny 2004; Moreno et al. 2012). Aside from the 928  
 929 increase in arid conditions, the intensification of 929  
 930 anthropogenic activity during this period also had a 930  
 931 strong impact on the forest and the environmental 931  
 932 variability in the region (Reille 1976; Benkaddour 932  
 933 1993) where significant anthropogenic alteration of 933  
 934 forest cover was recorded, especially in the last two 934  
 935 millennia (Cheddadi et al. 2015). However, coprophil- 935  
 936 ous fungal spore evidence in the Flowers Marsh 936  
 937 record did not indicate increased anthropogenic pres- 937  
 938 sure during this period. A high stand period was 938  
 939 recorded at Flowers Marsh from 650 to 150 cal. yr BP. 939  
 940 Considering the uncertainties of the chronological 940  
 941 model for this time interval, this phase could coincide 941  
 942 with the Little Ice Age (LIA), a generally cold period 942  
 943 (Mann et al. 2009). This short humid phase is 943  
 944 synchronous with decreased drought stress in the 944  
 945 Middle Atlas documented in *Cedrus atlantica* ring 945  
 946 width data (Esper et al. 2007) and in speleothem 946  
 947 records (Wassenburg et al. 2013). Cooling episodes 947  
 948 favoring the expansion of *Cedrus* were recorded 948  
 949 during this period at Tigalmamine Lake (Lamb et al. 949  
 950 1989) and in Aguelmam Sidi Ali sediments (Campbell 950  
 951 et al. 2017). 951

## 952 Conclusions

953 The multiproxy study (sedimentological, geochemi- 953  
 954 cal, mineralogical, biological—spores of coprophilous 954  
 955 fungi, ostracods and diatoms, and AMS <sup>14</sup>C dating), 955

956 carried out on the Flowers Marsh sedimentary  
957 sequence from the Middle Atlas region, provides a  
958 paleohydrological and paleoenvironmental recon-  
959 struction (of the area) since 6000 cal. yr BP, inter-  
960 preted in terms of climate and environment variability.  
961 This study demonstrates the ability of a pond such as  
962 Flowers Marsh to show significant palaeohydrological  
963 evolution and confirms the high sensitivity of Middle  
964 Atlas hydrosystems to climatic changes in the  
965 Mediterranean region as highlighted in previous  
966 studies.

967 The Flowers Marsh record shows arid conditions  
968 prior to 2300 cal. yr BP represented by highly clastic  
969 sediments and poor preservation of bioproxies. A large  
970 increase in water availability, marked by enhanced  
971 organic matter and endogenic calcite preservation was  
972 recorded during the wetter Iberian-Roman period,  
973 particularly between 2000 and 1400 cal. yr BP and  
974 during the Little Ice Age (650–150 cal. yr BP). Lower  
975 lake levels, a response to increasing regional aridity,  
976 were recorded during the Medieval Climate Anomaly  
977 (1400–650 cal. yr BP). Intensification of human  
978 pressure by pastures in the Flowers Marsh catchment  
979 is recorded since the last 150 year.

980 Comparison of the main hydrological phases in  
981 Flowers March with other Middle Atlas and Mediter-  
982 ranean records demonstrates a coherent pattern of the  
983 main climatic phases in the region during the last 6000  
984 years, at the same time highlighting spatial and  
985 temporal variability due to latitudinal differences  
986 and some site specific patterns.

987 **Acknowledgements** This study was funded by the French-  
988 Moroccan cooperation program PHC Toubkal/16/38 - Campus  
989 France: 34728VH. The authors also thank Mistrals/Paleomex  
990 and CNRST (Morocco) for financial support. Part of the  
991 Radiocarbon dating was performed at the LMC14 laboratory  
992 with the French ARTEMIS Program. D. Barboni is thanked for  
993 the preparation and observation of coprophilous fungi spore  
994 samples.

## 995 References

996 Adallal R, Vallet-Coulomb C, Vidal L, Benkaddour A, Ali  
997 Rhoujjati A, Sonzogni C (2019) Modelling lake water and  
998 isotope mass balance variations under Mediterranean cli-  
999 mate: Lake Azigza in the Moroccan Middle Atlas. *Reg*  
1000 *Environ Change* 19(8):2697–2709  
1001 Agnihotri R, Altabet MA, Herbert TD, Tierney JE (2008)  
1002 Subdecadally resolved paleoceanography of the Peru

margin during the last two millennia. *Geochem Geophys*  
1003 *Geosyst* 9:Q05013  
1004 Aitchison J (1982) The statistical analysis of compositional data.  
1005 *J Roy Stat Soc B Met* 44:139–177  
1006 Arz HW, Pätzold J, Müller PJ, Moammar MO (2003) Influence  
1007 of Northern Hemisphere climate and global sea level rise  
1008 on the restricted Red Sea marine environment during ter-  
1009 mination I. *Paleoceanography* 18:1053  
1010 Aufgebauer A, Panagiotopoulos K, Wagner B, Schaebitz F,  
1011 Viehberg FA, Vogel H, Zanchetta G, Sulpizio R, Leng MJ,  
1012 Damaschke M (2012) Climate and environmental change  
1013 over the last 17 ka recorded in sediments from Lake Prespa  
1014 (Albania/F.Y.R. of Macedonia/Greece). *Quatern Int*  
1015 274:122–135  
1016 Barker PA, Roberts N, Lamb HF, van der Kaars S, Benkaddour  
1017 A (1994) Interpretation of Holocene lake-level change  
1018 from diatom assemblages in Lake Sidi Ali, Middle Atlas,  
1019 Morocco. *J Paleolimnol* 12:223–234  
1020 Bell BA, Fletcher WJ, Cornelissen HL, Campbell JF, Ryan P,  
1021 Grant H, Zielhofer C (2019) Stable carbon isotope analysis  
1022 on fossil *Cedrus* pollen shows summer aridification in  
1023 Morocco during the last 5000 years. *J Quat Sci*  
1024 34(4–5):323–332  
1025 Benkaddour A (1993) Changements hydrologiques et clima-  
1026 tiques dans le Moyen-Atlas marocain; chronologie,  
1027 minéralogie, géochimie isotopique, et élémentaire des  
1028 sédiments lacustre de Tigalmamine. Thèse de l'Université  
1029 de Paris XI-France, p. 199  
1030 Benkaddour A, Lamb H, Leng M, Gasse F (2005) Stable isotope  
1031 records of Holocene environmental change from Moroccan  
1032 lakes: an emerging synthesis. [http://www.pages-igbp.org/  
1033 download/docs/meeting-products/posters/2005-osm2/  
1034 Benkaddour-A.pdf](http://www.pages-igbp.org/download/docs/meeting-products/posters/2005-osm2/Benkaddour-A.pdf) [26.01.2015]  
1035 Blaauw M (2010) Methods and code for 'classical' age-mod-  
1036 elling of radiocarbon sequences. *Quat Geochronol*  
1037 5:512–518  
1038 Born K, Fink AH, Knippertz P (2010) Dry and wet periods in the  
1039 northwestern Maghreb for present day and future climate  
1040 conditions. *Meteorol Z* 17(5):533–551  
1041 Bradley RS (2015) *Paleoclimatology: Reconstructing climates*  
1042 *of the Quaternary*. Amsterdam, Elsevier, pp 675  
1043 Brauer A (2004) Annually laminated lake sediments and their  
1044 palaeoclimatic relevance. In: Fischer H, Kumke T, Loh-  
1045 mann G, Flöser G, Miller G, von Storch H, Negendank  
1046 JFW (eds) *Towards a synthesis of Holocene proxy data and*  
1047 *ClimateModels*. Springer, Berlin, pp 109–128  
1048 Brisset E, Djamali M, Bard E, Borschneck D, Gandouin E,  
1049 Garcia M, Stevens L, Tachikawa K (2019) Late Holocene  
1050 hydrology of Lake Maharlou, Southwest Iran, inferred  
1051 from high-resolution sedimentological and geochemical  
1052 analyses. *J Paleolimnol* 61(1):111–128  
1053 Brown E, Johnson T, Scholz C, Cohen A, King J (2007) Abrupt  
1054 change in tropical African climate linked to the bipolar  
1055 seesaw over the past 55,000 years. *Geophys Res Lett*  
1056 34(20)  
1057 Campbell JFE, Fletcher WJ, Joannin S, Hughes PD, Rhanem M,  
1058 Zielhofer C (2017) Environmental Drivers of Holocene  
1059 forest development in the Middle Atlas, Morocco. *Front*  
1060 *Ecol Environ* 5(September):1–22  
1061

- 1062 Carrión JS (2002) Patterns and processes of Late Quaternary  
1063 environmental change in a montane region of southwestern  
1064 Europe. *Quaternary Sci Rev* 21:2047–2066
- 1065 Carrión JS, Fernández S, Jiménez-Moreno G, Fauquette S, Gil-  
1066 Romera G, González-Sampériz P, Finlayson C (2010) The  
1067 historical origins of aridity and vegetation degradation in  
1068 Southeastern Spain. *J Arid Environ* 74(7):731–736
- 1069 Cheddadi R, Lamb HF, Guiot J, Van Der Kaars S (1998)  
1070 Holocene climatic change in Morocco: A quantitative  
1071 reconstruction from pollen data. *Clim Dyn* 14(12):883–890
- 1072 Cheddadi R, Nourelbait M, Bouaissa O, Tabel J, Rhoujjati A,  
1073 López-Sáez JA, Alba-Sánchez F, Khater C, Ballouche A,  
1074 Dezileau L, Lamb H (2015) A history of human impact on  
1075 Moroccan Mountain landscapes. *Afr Archaeol Rev*  
1076 32:233–248
- 1077 Cheddadi R, Palmisano A, López-Sáez JA, Nourelbait M,  
1078 Zielhofer C, Tabel J, Rhoujjati A, Khater C, Woodbridge J,  
1079 Lucarini G, Broodbank C, Fletcher WJ, Roberts N (2019)  
1080 Human demography changes in Morocco and environ-  
1081 mental imprint during the Holocene. *Holocene*  
1082 29(5):816–829
- 1083 Chillasse L, Dakki M, Abbassi M (2001) Valeurs et fonctions  
1084 écologiques des zones humides du Moyen Atlas. *Humed*  
1085 *Mediterr* 1:139–146
- 1086 Corella JP, Moreno A, Morellón M, Rull V, Giralt S, Rico MT,  
1087 Pérez-Sanz A, Valero- Garcés BL (2011) Climate and  
1088 human impact on a meromictic lake during the last 6000  
1089 years (Montcortès Lake, Central Pyrenees, Spain). *J Pale-*  
1090 *olimnol* 46:351–367
- 1091 Corella JP, Stefanova V, El Anjoumi A, Rico E, Giralt S,  
1092 Moreno A, Plata-Montero A, Valero-Garcés BL (2013) A  
1093 2500-year multi-proxy reconstruction of climate change  
1094 and human activities in northern Spain: the Lake Arreo  
1095 record. *Palaeogeogr Palaeocl* 386:555–568
- 1096 Craig H (1965) The measurement of oxygen isotope  
1097 palaeotemperatures. In: Tongiorgi E (ed) *Stable isotopes in*  
1098 *oceanographic studies and palaeotemperatures*. Pisa,  
1099 Consiglio Nazionale delle Ricerche Laboratorio di  
1100 Geologia Nucleare, pp 161–182
- 1101 Croudace IW, Rindby A, Rothwell RG (2006) ITRAX:  
1102 description and evaluation of a new multi-function X-ray  
1103 core scanner. *Geol Soc Spec Publ London* 267(1):51–63
- 1104 Cugny C, Mazier F, Galop D (2010) Modern and fossil non-  
1105 pollen palynomorphs from the Basque mountains (western  
1106 Pyrenees, France): the use of coprophilous fungi to  
1107 reconstruct pastoral activity. *Veg Hist Archaeobot*  
1108 19:391–408
- 1109 Currás A, Zamora L, Reed JM, García-Soto E, Ferrero S,  
1110 Armangol X, Mezquita-Joanes F, Marqués MA, Riera S,  
1111 Julià R (2012) Climate change and human impact in central  
1112 Spain during Roman times: high-resolution multi-proxy  
1113 analysis of a tufa lake record (Somolinos, 1280 m asl).  
1114 *Catena* 89:31–53
- 1115 Damnati B, Etebaai I, Benjlani H, El Khoudri K, Reddad H,  
1116 Taieb M (2015) Sedimentology and geochemistry of  
1117 lacustrine terraces of three Middle Atlas lakes: paleohy-  
1118 drological changes for the last 2300 cal BP in Morocco  
1119 (western Mediterranean region). *Quatern Int* 404:163–173
- 1120 Davies SJ, Lamb HF, Roberts SJ (2015) Micro-XRF core  
1121 scanning in palaeolimnology: recent developments. In:  
Micro-XRF studies of sediment cores. Springer, Dordrecht,  
pp 189–226
- Davis OK, Schafer D (2006) *Sporormiella* fungal spores, a  
palynological means of detecting herbivore density.  
*Palaeogeogr Palaeocl* 237:40–50
- Develle AL, Herreros J, Vidal L, Surssock A, Gasse F (2010)  
Controlling factors on a paleo-lake oxygen isotope record  
(Yammoûneh, Lebanon) since the Last Glacial Maximum.  
*Quat Sci Rev* 29(7–8):865–886
- Di Rita F, Fletcher WJ, Aranbarri J, Margaritelli G, Lirer F,  
Magri D (2018) Holocene forest dynamics in central and  
western Mediterranean: periodicity, spatio-temporal pat-  
terns and climate influence. *Sci Rep-UK* 8(1):1–13
- Epstein S, Buchsbaum R, Lowenstam HA et Urey HC (1953)  
Echelle de température isotopique révisée eau-carbonate.  
*Bull Soc Géol Amérique* 64(11):1315–1326
- Esper J, Frank D, Büntgen U, Verstege A, Luterbacher J,  
Xoplaki E (2007) Long-term drought severity variations in  
Morocco. *Geophys Res Lett* 34:L17702
- Espitalié J, Laporte JL, Madec M, Marquis F, Leplat P, Paulet J,  
Boutefeu A (1977) Méthode rapide de caractérisation des  
roches-mère, de leur potentiel pétrolier et de leur degré  
d'évolution. *Rev Inst Franc Petrol* (32): 23–42
- Etebaai I, Damnati B, Raddad H, Benhardouz H, Benhardouz O,  
Miche H, Taieb M (2012) Impacts climatiques et anthro-  
piques sur le fonctionnement hydrogéochimique du Lac  
Ifrah (Moyen Atlas marocain). *Hydrol Sci J* 57(3):547–561
- Fægri K, Iversen J (1989) *Textbook of pollen analysis*. Wiley,  
Chichester-New York-Brisbane-Toronto-Singapore
- Flower RJ, Foster IDL (1992) Climatic implications of recent  
changes in lake level at Lac Azizga (Morocco). *Bull Soc*  
*Géol France* 163:91–96
- Flower RJ, Stevenson AC, Dearing JA, Foster ID, Airey A,  
Rippey B, Wilson JPF, Appleby PG (1989) Catchment  
disturbance inferred from paleolimnological studies of  
three contrasted sub-humid environments in Morocco.  
*J Paleolimnol* 1:293–322
- Ghasemi A, Zahediasl S (2012) Normality tests for statistical  
analysis: a guide for non-statisticians. *Int J Endocrinol*  
10:486–489
- Gilfedder BS, Petri M, Wessels M, Biester H (2011) Bromine  
species fluxes from Lake Constance's catchment and a  
preliminary lake mass balance. *Geochim Cosmochim Acta*  
75:3385–3401
- Giorgi F (2006) Climate change hot-spots. *Geophys Res Lett*  
33(8):L08, 707
- González-Sampériz P, Valero-Garcés BL, Moreno A, Morellón  
M, Navas A, Machin J, Delgado-Huertas A (2008) Vegeta-  
tion changes and hydrological fluctuations in the Central  
Ebro Basin (NE Spain) since the Late Glacial period: saline  
lake records. *Palaeogeogr Palaeocl* 259:136–115
- Harell Jr, Frank E, Dupont C (2006) *Le paquet Hmisc*. Version  
du package R, 3 (0–12), 3
- Hinaje S, Ait Brahim L (2002) Les bassins lacustres du Moyen  
Atlas (Maroc): un exemple d'activité tectonique poly-  
phasée associée à des structures d'effondrement. *Comu-  
nicações do Instituto Geológico e Mineiro* 89:283–294
- Interlandi SJ, Kilham SS (2001) Limiting resources and the  
regulation of diversity in phytoplankton communities.  
*Ecology* 82:1270–1282

- 1182 Jalut G, Dedoubat JJ, Fontugne M, Otto T (2009) Holocene  
1183 circum-Mediterranean vegetation changes: climate forcing  
1184 and human impact. *Quatern Int* 200:4–18 1244
- 1185 Jiménez-Moreno G, Rodríguez-Ramírez A, Pérez-Asensio JN,  
1186 Carrión JS, López-Sáez JA, Villarías-Robles JJ, Celestino-  
1187 Pérez S, Cerrillo-Cuenca E, León A, Contreras C (2015)  
1188 Impact of late-Holocene aridification trend, climate vari-  
1189 ability and geodynamic control on the environment from a  
1190 coastal area in SW Spain. *Holocene* 25(4):607–617 1246
- 1191 Jouve G, Vidal L, Adallal R, Rhoujjati A, Benkaddour A,  
1192 Chapron E, Tachikawa K, Bard E, Courp T, Dezileau L,  
1193 Hebert B, Rapuc W, Simonneau A, Sonzogni C, Sylvestre  
1194 S (2019) Recent hydrological variability of the Moroccan  
1195 Middle-Atlas Mountains inferred from micro-scale sedi-  
1196 mentological and geochemical analyses of lake sediments.  
1197 *Quat Res* 91(1):414–430 1247
- 1198 Kalugin I, Daryin A, Smolyaninova L, Andreev A, Diekmann B,  
1199 Khlystov O (2007) 800-yr-long records of annual air  
1200 temperature and precipitation over southern Siberia infer-  
1201 red from Teletskoye Lake sediments. *Quatern Int*  
1202 67:400–410 1248
- 1203 King A, Eckersley R (2019) Statistics for biomedical engineers  
1204 and scientists: how to visualize and analyze data. Aca-  
1205 demic Press, Cambridge 1249
- 1206 Krammer K, Lange-Bertalot H (1986–1991) Bacillariophyceae.  
1207 Süßwasserflora von Mitteleuropa, 2/1–2/4. G. Fischer  
1208 Verlag, Stuttgart 1250
- 1209 Kylander M, Ampel L, Wohlfarth B, Veres D (2011) High-  
1210 resolution X-ray fluorescence core scanning analysis of Les  
1211 Echets (France) sedimentary sequence: new insights from  
1212 chemical proxies. *J Quat Sci* 26:109–117 1251
- 1213 Lamb HF, Eicher U, Switsur VR (1989) An 18,000-Year record  
1214 of vegetation, lake-level and climatic change from Tigal-  
1215 mamine, Middle Atlas, Morocco. *J Biogeogr* 16(1):65–74 1252
- 1216 Lamb HF, Roberts N, Leng M, Barker PH, Benkaddour A, Van  
1217 Der Kaars S (1999) Lake evolution in a semi-arid mountain  
1218 environment: response to catchment change and hydroclim-  
1219 atic variation. *J Paleolimnol* 21(3):325–343 1253
- 1220 Lamb HF, van der Kaars S (1995) Vegetational response to  
1221 Holocene climatic change: pollen and palaeolimnological  
1222 data from the Middle Atlas, Morocco. *The Holocene*  
1223 5(4):400–408 1254
- 1224 Macklin MG, Benito G, Gregory KJ, Johnstone E, Lewin J,  
1225 Michezyńska DJ, Soja R, Starkel L, Thorndycraft VR  
1226 (2006) Past hydrological events reflected in the Holocene  
1227 fluvial record of Europe. *Catena* 66:145–154 1255
- 1228 Magny M (1992) Sédimentation et dynamique de comblement  
1229 dans les lacs du jura au cours des 15 derniers millénaires.  
1230 *Revue d'Archéométrie* 16:27–49 1256
- 1231 Magny M (2004) Holocene climate variability as reflected by  
1232 mid-European lake-level fluctuations and its probable  
1233 impact on prehistoric human settlements. *Quat Int*  
1234 113:65–79 1257
- 1235 Mann ME, Zhang Z, Rutherford S, Bradley RS, Hughes MK,  
1236 Shindell D, Ammann C, Faluvegi G, Ni F (2009) Global  
1237 signatures and dynamical origins of the Little Ice Age and  
1238 Medieval Climate Anomaly. *Science* 326:1256–1260 1258
- 1239 Marciniak B (1986) Late glacial *Fragilaria* flora from lake  
1240 sediments of the Tatra Mts. and the Alps. In: Round FE  
1241 (1988) Proceedings of the Ninth International Diatom  
1242 Symposium: Bristol, August 24–30, 1986. Biopress Lim-  
1243 itted pp 233–243 1244
- Marcott SA, Shakun JD, Clark PU, Mix AC (2013) A recon-  
1245 struction of regional and global temperature for the past  
1246 11,300 years. *Science* 339:1198–1201 1247
- Martin J (1981) Le Moyen Atlas Central: étude géomor-  
1248 phologique. Notes et Mémoires du Service Géologique du  
1249 Maroc, Rabat: Editions du service géologique du Maroc,  
1250 No. 258 bis, 1–447 1251
- Martín-Puertas C, Valero-Garcés BL, Brauer A, Mata MP,  
1252 Delgado-Huertas A, Dulski P (2009) The Iberian–Roman  
1253 humid period (2600–1600 cal yr BP) in the Zoñar Lake  
1254 varve record (Andalucía, southern Spain). *Quat Res*  
1255 71:108–120 1256
- Martín-Puertas C, Valero-Garcés BL, Mata MP, González-  
1257 Sampérez P, Bao R, Moreno A, Stefanova V (2008) Arid  
1258 and humid phases in southern Spain during the last 4000  
1259 years: the Zoñar Lake record, Cordoba. *Holocene*  
1260 18(6):907–921 1261
- Martín-Puertas C, Valero-Garcés BL, Mata MP, Moreno A,  
1262 Giralt S, Martínez-Ruiz F, Jiménez-Espejo F (2011) Geo-  
1263 chemical processes in a Mediterranean Lake: a high-reso-  
1264 lution study of the last 4,000 years in Zonar Lake, southern  
1265 Spain. *J Paleolimnol* 46(3):405–421 1266
- McKenzie JA (1985) Carbon isotopes and productivity in the  
1267 lacustrine and marine Environment. In: Stumm W (ed)  
1268 Chemical processes in lakes. Wiley, New York, pp 99–118 1269
- Meisch C (2000) Freshwater Ostracoda of western and central  
1270 Europe. Spektrum Akademischer Verlag, Heidelberg,  
1271 p 522 1272
- Morellón M, Valero-Garcés BL, Moreno A, González-Sampérez  
1273 P, Mata P, Romero O, Maestro M, Navas A (2008) Holo-  
1274 cene palaeohydrology and climate variability in North-  
1275 eastern Spain: the sedimentary record of lake Estanya (Pre-  
1276 Pyrenean range). *Quatern Int* 181:15–31 1277
- Moreno A, Pérez A, Frigola J, Nieto-Moreno V, Rodrigo-Gámiz  
1278 M, Martrat B, González-Sampérez P, Morellón M, Martín-  
1279 Puertas C, Corella JP, Belmonte A, Sancho C, Cacho I,  
1280 Herrera G, Canals M, Grimalt JO, Jiménez-Espejo F,  
1281 Martínez-Ruiz F, Vegas-Vilarrúbia T, Valero-Garcés BL  
1282 (2012) The Medieval climate anomaly in the Iberian  
1283 Peninsula reconstructed from marine and lake records.  
1284 *Quat Sci Rev* 43:16–32 1285
- Nour El Bait M, Rhoujjati A, Benkaddour A, Carré M, Eynaud  
1286 F, Martinez P, Cheddadi R (2016) Climate change and  
1287 ecosystems dynamics over the last 6000 years in the  
1288 Middle Atlas, Morocco. *Clim Past* 12:1029–1042 1289
- Nour El Bait M, Rhoujjati A, Eynaud F, Benkaddour A, Dezi-  
1290 leau L, Wainer K, Goslar T, Khater C, Tabel J, Cheddadi R  
1291 (2014) An 18 000-year pollen and sedimentary record from  
1292 the cedar forests of the Middle Atlas, Morocco. *J Quat Sci*  
1293 29(5):423–432 1294
- Olsen J, Anderson JN, Knudsen MF (2012) Variability of the  
1295 North Atlantic Oscillation over the past 5200 years. *Nat*  
1296 *Geosci* 5:808–812 1297
- Reille M (1976) Analyse pollinique de sédiments postglaciaires  
1298 dans le Moyen-Atlas et le Haut- Atlas marocains: premiers  
1299 résultats. *Ecol Mediterr* 2:153–170 1300
- Reimer PJ, Bard E, Bayliss A, Beck JW, Blackwell PG, Bronk  
1301 Ramsey C, Buck CE, Cheng H, Edwards RL, Friedrich M,  
1302 Grootes PM, Guilderson TP, Hafflidson H, Hajdas I, Hatté

- 1303 C, Heaton TJ, Hoffmann DL, Hogg AG, Hughen KA, 1360  
 1304 Kaiser KF, Kromer B, Manning SW, Niu M, Reimer RW, 1361  
 1305 Richards DA, Scott EM, Southon JR, Staff RA, Turney 1362  
 1306 CSM, van der Plicht J (2013) IntCal13 and Marine13 1363  
 1307 radiocarbon age calibration curves 0–50,000 years cal BP. 1364  
 1308 Radiocarbon 55(4):1869–1887 1365  
 1309 Rhoujjati A, Cheddadi R, Taieb M, Baali A, Ortu E (2010) Past 1366  
 1310 environmental changes during the last 25,000 years in the 1367  
 1311 Middle Atlas (Morocco): A record from lake Ifrah. J Arid 1368  
 1312 Environ 74(7):737–745 1369  
 1313 Rhoujjati A, Nourelbait M, Benkaddour A, Damnati B, Baali A, 1370  
 1314 Taieb M, Decobert M, Malek F, Cheddadi R (2012) 1371  
 1315 Palaeoenvironmental context inferred from Holocene 1372  
 1316 deposits of lake Iffer (Middle Atlas, Morocco). Quaternaire 1373  
 1317 23(3):241–252 1374  
 1318 Roberts N, Jones MD, Benkaddour A, Eastwood WJ, Filippi 1375  
 1319 ML, Frogley MR, Lamb HF, Leng MJ, Reed JM, Stein M, 1376  
 1320 Stevens L, Valero-Garcés B, Zanchetta G (2008) 1377  
 1321 Stable isotope records of Late Quaternary climate and 1378  
 1322 hydrology from Mediterranean lakes: the ISOMED syn- 1379  
 1323 thesis. Quat Sci Rev 27:2426–2441 1380  
 1324 Saadi M, Maroc. Direction des mines et de la géologie, et 1381  
 1325 Maroc. Service géologique (1982) Carte structurale du 1382  
 1326 Maroc. Service géologique du Maroc 1383  
 1327 Santos L, Vidal Romani JR, Jalut G (2000) History of vegetation 1384  
 1328 during the Holocene in the Courel and Queixa Sierras, 1385  
 1329 Galicia, Northwest Iberian Peninsula. J Quat Sci 1386  
 1330 15:621–632 1387  
 1331 Sayad A, Chakiri S (2010) Impact de l'évolution du climat sur le 1388  
 1332 niveau de Dayet Aoua dans le Moyen Atlas marocain. 1389  
 1333 Science et changements planétaires/Sécheresse 1390  
 1334 21(4):245–251 1391  
 1335 Sayad A, Chakiri S, Martin C, Bejjaji Z, Echarfaoui H (2011) 1392  
 1336 Effet des conditions climatiques sur le niveau du lac Sidi 1393  
 1337 Ali (Moyen Atlas, Maroc). Physio-Géo Géographie phy- 1394  
 1338 sique et environnement, (Volume 5), 251–268 1395  
 1339 Solomon S, Plattner G, Knutti R, Friedlingsteind P (2009) 1396  
 1340 Irreversible climate change due to carbon dioxide emis- 1397  
 1341 sions. P Natl A Sci 106(6):1704–1709 1398  
 1342 Soulié-Marsche I, Benkaddour A, El Khiati N, Gemayel P, 1399  
 1343 Ramdani M (2008) Charophytes, indicateurs de paléo- 1400  
 1344 bathymétrie du lac Tigalmamine (Moyen Atlas, Maroc). 1401  
 1345 Geobios 41:435–444 1402  
 1346 Stockmarr J (1971) Tablets with spores used in absolute pollen 1403  
 1347 analysis. Pollen Spore 13:615–621 1404  
 1348 Stuiver M (1970) Oxygen and carbon isotope ratios of fresh- 1405  
 1349 water carbonates as climatic indicators. J Geophys Res 1406  
 1350 75:5247–5257 1407  
 1351 Tabel J, Khater C, Rhoujjati A, Dezileau L, Bouimetarhan I, 1408  
 1352 Carre M, Vidal L, Benkaddour A, Nourelbait M, Cheddadi 1409  
 1353 R (2016) Environmental changes over the past 25000 years 1410  
 1354 in the southern Middle Atlas, Morocco. J Quat Sci 1411  
 1355 31(2):93–102 1412  
 1356 Thió-Henestrosa S, Martín-Fernández JA (2006) Detailed guide 1413  
 1357 to CoDaPack: a freeware compositional software. Com-  
 1358 positional Compositional data analysis in the geosciences:  
 1359 from theory to practice, Buccianti A, Mateu-Figueras G,  
 Pawlowsky-Glahn V (eds) Geol Soc Spec Publ, London  
 264(1): pp 101–118  
 Valero-Garcés BL (ed) (2003) Limnogeologia en España: Un  
 Tributoa Kerry Kelts (Vol. 14). Editorial CSIC-CSIC Press  
 Valero-Garcés BL, Navas A, Machin J, Stevenson T, Davis B  
 (2000) Responses of a saline lake ecosystem in a semiarid  
 region to irrigation and climate variability: the history of  
 Salada Chiprana, Central Ebro Basin, Spain. Ambio,  
 344–350  
 Van Geel B (2002) Non-pollen palynomorphs. In: Smol JD,  
 Birks JB, Last WM (eds) Tracking environmental change  
 using lake sediments, vol 3. Terrestrial, algal, and siliceous  
 indicators Kluwer, Dordrecht, pp 99–119  
 Vidal L, Rhoujjati A, Adallal R, Jouve G, Bard E, Benkaddour  
 A, Chapron E, Courp T, Dezileau L, Garcia M, Hebert B,  
 Simmoneau A, Sonzogni C, Sylvestre F, Tachikawa K,  
 ValletCoulomb C, Viry E (2016) Past hydrological vari-  
 ability in the Moroccan Middle Atlas inferred from lakes  
 and lacustrine sediments. In: Sabrié M-L, Gibert-Brunet E,  
 Mourier T (eds) The Mediterranean Region under climate  
 change. IRD, AllEnvi, pp 57–69  
 Wassenburg JA, Immenhauser A, Richter DK, Niedermayr A,  
 Riechelmann S, Fietzke J, Scholz D, Jochum KP,  
 Fohlmeister J, Schröder-Ritzrau A, Sabaoui A (2013)  
 Moroccan speleothem and tree ring records suggest a  
 variable positive state of the North Atlantic Oscillation  
 during the Medieval warm period. Earth Planet Sci Lett  
 375:291–302  
 Wei T, Simko V, Levy M, Xie Y, Jin Y, Zeng J (2017) Package  
 'corrplot'. Statistician 56:316–324  
 Weltje GJ, Bloemsa MR, Tjallingii R, Heslop D, Röhl U,  
 Croudace IW (2015) Prediction of geochemical composi-  
 tion from XRF core scanner data: a new multivariate  
 approach including automatic selection of calibration  
 samples and quantification of uncertainties. In: Croudace  
 IW, Rothwell RG (eds) Micro XRF Studies of sediment  
 cores (DPER 17). Springer, Dordrecht, pp 507–534  
 Williams JJ, Gosling WD, Coe AL, Brooks SJ, Gulliver P (2011)  
 Four thousand years of environmental change and human  
 activity in the Cochabamba Basin, Bolivia. Quat Res  
 76:58–68  
 Xia J, Ito E, Engstrom DR (1997) Geochemistry of ostracode  
 calcite: Part 1. An experimental determination of oxygen  
 isotope fractionation. Geochim Cosmochim Acta  
 61(2):377–382  
 Zielhofer C, Fletcher WJ, Mischke S, Batist M, De Campbell  
 JFE, Joannin S, Tjallingii R, El Hamouti N, Junginger A,  
 Stele A, Bussmann J, Schneider B, Lauer T, Spitzer K,  
 Strupler M, Brachert T, Mikdad A (2017) Atlantic forcing  
 of Western Mediterranean winter rain minima during the  
 last 12,000 years. Quaternary Sci Rev 157:29–51  
 Zolitschka B (2007) Varved lake sediments. In: Elias SA (ed)  
 Encyclopedia of quaternary science. Elsevier, Amsterdam,  
 pp 3105–3114

Journal : **10933**

Article : **166**

## Author Query Form

**Please ensure you fill out your response to the queries raised below and return this form along with your corrections**

Dear Author

During the process of typesetting your article, the following queries have arisen. Please check your typeset proof carefully against the queries listed below and mark the necessary changes either directly on the proof/online grid or in the 'Author's response' area provided below

Query	Details Required	Author's Response
<a href="#">AQ1</a>	Please check and confirm the edit in Article title.	